Unmasking Hidden Systemic Effects of Neurodegenerative Diseases: A Two-Pronged Approach to Biomarker Discovery

Sandra I. Anjo[1,2,3,4,*,†], Miguel Rosado[1,2,3,5,*], Inês Baldeiras[1,2,6], Andreia Gomes[7], Diana Pires[7], Cátia Santa[1,2,3], Joana Pinto[1,2], Cristina Januário[6], Isabel Santana[1,2,6], Ana Verdelho[8,9], Alexandre de Mendonça[9], Miguel Castelo-Branco[7,#], Bruno Manadas[1,2,3#,†]

[1] CNC - Centro de Neurociências e Biologia Celular, Universidade de Coimbra, Rua Larga - Faculdade de Medicina, 1ºandar - POLO I, 3004-504 Coimbra, Portugal.

[2] CIBB - Centre for Innovative Biomedicine and Biotechnology, University of Coimbra, Rua Larga - Faculdade de Medicina, 1ºandar - POLO I, 3004-504 Coimbra, Portugal.

[3] Instituto de Investigação Interdisciplinar, Universidade de Coimbra (IIIUC), Casa Costa Alemão, R. Dom Francisco de Lemos, 3030-789 Coimbra, Portugal.

[4] Faculdade de Medicina, Universidade de Coimbra, Azinhaga de Santa Comba, 3000-548 Coimbra, Portugal.

[5] - University of Coimbra, Institute for Interdisciplinary Research, Doctoral Programme in Experimental Biology and Biomedicine (PDBEB), Portugal

[6] Serviço de Neurologia, Centro Hospitalar e Universitário de Coimbra, Praceta Professor Mota Pinto, 3004-561 Coimbra, Portugal.

[7] Coimbra Institute for Biomedical Imaging and Translational Research (CIBIT), Azinhaga de. Santa Comba, 3000-548 Coimbra, Portugal.

[8] Department of Neurosciences and Mental Health, Santa Maria Hospital - CHLN, ISAMB, University of Lisbon, Av. Prof. Egas Moniz MB, 1649-028 Lisboa, Portugal.

[9] Instituto de Medicina Molecular e Faculdade de Medicina, Universidade de Lisboa, Av. Prof. Egas Moniz, 1649-028 Lisboa, Portugal.

* - Equal contribution

# - Senior equal contribution

† - Corresponding authors: Bruno Manadas (bmanadas@cnc.uc.pt, +351231249170) and Sandra Anjo (sandra.anjo@cnc.uc.pt, +351231249170), Center for Neuroscience and Cell Biology – University of Coimbra, UC Biotech - Parque Tecnológico de Cantanhede, Núcleo 04, Lote 8, 3060-197 Cantanhede – Portugal

E-mail addresses: Miguel Rosado - mmva.rosado@gmail.com; Ines Baldeiras - ibaldeiras@cnc.uc.pt; Andreia Gomes - andmaggomes@gmail.com; Diana Pires - diana.santos.pires@gmail.com; Cátia Santa - catiajmsanta@gmail.com; Joana Pinto - joana.amaralpinto@gmail.com; Cristina Januário - cristinajanuario@gmail.com; Isabel Santana - isabeljsantana@gmail.com; Ana Verdelho - averdelho@medicina.ulisboa.pt; Alexandre de Mendonça - mendonca@medicina.ulisboa.pt; Miguel Castelo-Branco - mcbranco@fmed.uc.pt.

Abstract

Background: The identification of reliable blood biomarkers for neurodegenerative Diseases (NDs) has been of pivotal importance in translational/clinical research. However, conventional omics struggle with the complexity of blood samples, which makes it difficult to achieve the desired goal. To address this, in this work the potential of High Molecular Weight (HMW) fractionation under non-denaturing conditions as a complementary approach to the conventional proteomics for identifying serum biomarkers in NDs was explored.

Methods: A cohort of 58 serum samples of Alzheimer's disease (AD), Parkinson's disease (PD) patients and control (CT) individuals was used to compare the two proteomics strategies: i) direct analysis of whole serum and ii) non-denaturing fractionation using 300 kDa cut-off filters (HMW serum). Univariate analysis was applied to the proteins quantified by each approach to identify the subset of proteins altered among the different groups (AD, PD and CT). Subsequently, linear discriminant analysis was performed using each subset of differently altered proteins, either individually or in combination, to construct the predictive models for the diseases under study and to identify a panel of potential biomarkers that could aid in the diagnosis of AD and PD.

Results: Although both approaches quantified a similar set of proteins, it was observed that each approach capture a distinct subset of differentially altered proteins, suggesting that HMW fractionation is capable of identifying additional types of alterations beyond conventional protein level changes. The discriminant model created by combining altered proteins from both datasets demonstrated an impressive efficacy in distinguishing between the three groups (AUC = 0.999 and, median sensitivity and specificity of 97.4% and 91.7%, respectively). Importantly, this performance surpassed that of any model created using each method individually.

Conclusions: Altogether, this work demonstrated that HMW fractionation can be a valuable complementary method to direct serum analysis and could enhance biomarker discovery. The 10 proteins included in the model (5 from each strategy), comprise clear evidence for the contribution of apolipoproteins for the diagnosis of NDs, revealing potential changes within lipid metabolism and the

62 organization of macromolecules and their complexes, thereby uncovering effects that remain hidden
63 from a conventional serum proteome analysis.

64 **Keywords**

65 Serum Proteomics

66 High Molecular Weight Fractionation

67 Neurodegenerative Diseases

68 SWATH-MS/DIA

69 Protein complexes/Proteoforms

70 Apolipoproteins

71 Lipoproteins

72 **Background**

73 Proteins can be directly or indirectly related to a myriad of diseases, thereby being important targets of
74 biomarker research, which remains a pivotal aspect of clinical research. However, biomarker discovery
75 based on conventional proteomics strategies has not yet yielded substantial practical applications. Blood
76 and its fractions are the most studied samples for biomarker identification, not only due to easy
77 accessibility but also because of its interactions with most tissues in the body, potentially reflecting
78 disease-related alterations (1, 2). However, both plasma and serum proteomes have a large dynamic
79 range of protein concentrations (1), with the detection of those least abundant being masked by the
80 most abundant. Despite all the technical developments in proteomics quantification by mass
81 spectrometry (MS) (3), the high dynamic range still precludes the complete characterization of these
82 samples, which may be one of the reasons why the identification of relevant biomarkers in
83 plasma/serum by MS remains challenging (4). Therefore, it is essential to have alternative approaches to
84 the direct analysis of these highly demanding biofluids. Several approaches have been developed to
85 reduce sample complexity (5), such as size exclusion chromatography and electrophoretic separation
86 methods. When dealing with numerous samples, a more straightforward approach that could serve as
87 an alternative to direct sample analysis is centrifugal ultrafiltration (5). This approach relies on the
88 separation of sample components based on size exclusion, which is correlated to molecular weight
89 (MW). This method has typically been used to study the low molecular weight proteome of serum and
90 plasma samples, using filters between 20 kDa and 40 kDa (6, 7), but it may also be used to study other
91 proteome fractions. Alzheimer's Disease (AD) and Parkinson's Disease (PD) are inherently linked to
92 protein aggregation (8) and, therefore, to the formation of high molecular weight (HMW) protein
93 complexes. Fractionation of peripheral fluid samples from patients with these diseases, focused on the
94 HMW proteome, could be useful to eliminate high abundance proteins and to study protein aggregates
95 that may be present in circulation. In this study, we propose using centrifugal ultrafiltration focused on
96 the HMW proteome, not as an alternative but as a complementary analysis to the investigation of
97 unfractionated samples, to potentially assess the restructuring of molecular complexes as a distinctive
98 feature of disease. To evaluate our hypothesis, the same set of samples was subjected to the
99 proteomics analysis of the whole serum and fractionation using centrifugal ultrafiltration with 300 kDa

100 molecular weight cut-off (MWCO) filters in a non-denaturing environment (henceforth referred to as
101 HMW fractionation). The data obtained from both approaches were directly compared and merged to
102 identify potential biomarkers. This study used a cohort consisting of patients with neurodegenerative
103 disorders, specifically Alzheimer's and Parkinson's disease patients, and healthy controls (CT) to test the
104 significance of using HMW fractionation as a complementary tool for biomarker discovery. These
105 disorders were chosen as they are considered as potential proteinopathies, making them promising
106 targets for this research.

107 ## Methods

108 ### Participants

109 A total of 58 serum samples were used in this study, comprising 3 groups of individuals: AD (n = 22), PD
110 (n = 24), and CT (n = 12). The PD patients were recruited at the Movement Disorders Units of the
111 Neurological Department of the CHUC, where they were assessed by a movement disorders specialist
112 and were diagnosed according to the criteria defined by the UK Parkinsons's Disease Society Brain Bank
113 (9). The exclusion criteria for these patients consisted of severe dementia (as indicated by a Mini-Mental
114 State Exam score below 15), any psychiatric disorder, or other forms of Parkinsonism. The clinical group
115 of individuals with AD diagnosis was recruited and prospectively evaluated by two experienced
116 neurologists at Memoclínica and the Neurology Department of the CHUC. The standard criteria for the
117 diagnosis of AD were the Diagnostic and Statistical Manual of Mental Disorders—fourth edition (DSM-
118 IV-TR) (10) and the National Institute on Aging and the Alzheimer's Association Workgroup (11). To
119 ensure the homogeneity of the sample, only patients who met the following criteria were included: they
120 were in a stable condition, did not sustain recent changes in medication, and did not have
121 ophthalmological or neurological/psychiatric conditions other than AD. The CT group was composed of
122 age- and gender-matched individuals from the community with no history of cognitive deterioration,
123 neurological or acquired central nervous system (CNS) disorders, traumatic brain injury, or psychiatric
124 disorders. The CT group was also submitted to a brief cognitive assessment to exclude the presence of
125 cognitive impairment.

126 ### Serum processing for proteomics analysis

127 Two different strategies were used to obtain a more comprehensive proteomic characterization of
128 serum samples, namely: i) direct analysis of whole serum and ii) HMW fractionation through
129 ultrafiltration using 300 kDa cut-off filters (HMW serum).

130 For each sample, 5 µL were used for direct serum analysis and 82.5 µL for HMW serum fractionation.
131 Additionally, three sample pools were prepared by combining aliquots of all the samples, for the AD
132 pool, PD pool, and CT pool, respectively. Pooled samples were used for Data-dependent acquisition

133 (DDA) experiments to build a specific protein library to be used in data-independent acquisition (DIA)
134 analysis and were subjected to the same sample processing as the individual samples. Before
135 processing, all samples were spiked with the same amount of an internal standard (IS) to account for
136 sample loss (12). Different internal standards were used depending on the type of analysis: MBP-GFP
137 (12) in the case of the whole serum approach, while equine ferritin, commonly available as one of the
138 standards in the Gel Filtration Calibrants Kit for High Molecular Weight proteins (GE28-4038-42), for the
139 HMW fractionation approach.

140 For the direct analysis of whole serum, the samples were diluted in Laemmli buffer, followed by
141 denaturation for 5 min at 95°C and cysteine alkylation with acrylamide, and the total volume in all
142 samples was subjected to in-gel digestion using the Short-GeLC for subsequent quantitative analysis by
143 LC-MS/MS-DIA (13).

144 Samples subjected to HMW fractionation were ultrafiltrated using 300 kDa cut-off filters (Vivaspin® 500
145 Polyethersulfone, 300 kDa (Sartorius)) pre-conditioned to PBS. Serum samples were diluted into 200 µL
146 of PBS and subjected to 20 min centrifugation at 14,500× g at 4 °C followed by an additional washing
147 step with another 200 µL of PBS. In some cases, the washing step was repeated until the retentate
148 volume did not exceed 50 µL. The resulting retentates, the HMW fraction, were collected into a new
149 LoBind® microcentrifuge tube and precipitated with ice-cold acetone (14). The precipitated pellets were
150 resuspended into 30 µL of a solution containing 2% SDS (v/v) and 1 M of Urea, always aided by
151 sonication (VibraCell 750 watt-Sonics ®) with ice in the cup horn (2 min. pulse duration, at 1 second
152 intervals, and with 40% amplitude). Afterward, concentrated Laemmli Buffer was added to the samples,
153 followed by a 30 min incubation to reduce the samples and a 20 min incubation with iodoacetamide for
154 cysteine alkylation (15). The total volume in all samples was subjected to in-gel digestion as previously
155 specified (13).

156 **Mass spectrometry data acquisition**

157 Samples were analyzed on a NanoLC™ 425 System (Eksigent®) couple to a TripleTOF™ 6600 System
158 (Sciex®) using DDA for each fraction of the pooled samples for protein identification and SWATH-MS
159 acquisition of each sample for protein quantification. Peptides were resolved by micro-flow liquid

160 chromatography on a MicroLC column ChromXP™ C18CL (300 µm ID × 15 cm length, 3 µm particles, 120
161 Å pore size, Eksigent®) at 5 µL/min. The liquid chromatography program was performed as follows with
162 a multistep gradient: 2 % to 5 % mobile phase B (0-2 min), 5 % to 28 % B (2-50 min), 28% to 35% B (50-
163 51 min), 35 to 98% of B (50–52 min), 98% of B (52-61 min), 98 to 2% of B (61–62 min), 2% of B (68 min).
164 Mobile phase A was composed of 0.1 % formic acid (FA) with 5% dimethyl sulfoxide (DMSO), and mobile
165 phase B was composed of 0.1 % FA and 5% DMSO in acetonitrile. Peptides were eluted into the mass
166 spectrometer using an electrospray ionization source (DuoSpray™ Source, ABSciex®) with a 25 µm
167 internal diameter hybrid PEEKsil/stainless steel emitter (ABSciex®). The ionization source was operated
168 in the positive mode set to an ion spray voltage of 5 500 V, 25 psi for nebulizer gas 1 (GS1) and 25 psi for
169 the curtain gas (CUR).

170 For DDA experiments, the mass spectrometer was set to scan full spectra (m/z 350-1250) for 250 ms,
171 followed by up to 100 MS/MS scans (m/z 100–1500) per cycle to maintain a cycle time of 3.309 s. The
172 accumulation time of each MS/MS scan was adjusted in accordance with the precursor intensity
173 (minimum of 30 ms for precursor above the intensity threshold of 1000). Candidate ions with a charge
174 state between +2 and +5 and counts above a minimum threshold of 10 counts per second were isolated
175 for fragmentation and one MS/MS spectrum was collected before adding those ions to the exclusion list
176 for 25 seconds (mass spectrometer was operated by Analyst® TF 1.7, ABSciex®). The rolling collision
177 energy (CE) was used with a collision energy spread (CES) of 5.

178 For SWATH-MS-based experiments, the mass spectrometer was operated in a looped product ion mode
179 (16) and the same chromatographic conditions were used as in the DDA experiments described above. A
180 set of 60 windows of variable width (containing 1 m/z for the window overlap) was constructed,
181 covering the precursor mass range of m/z 350-1250. A 250 ms survey scan (m/z 350-1500 m/z) was
182 acquired at the beginning of each cycle for instrument calibration and SWATH-MS/MS spectra were
183 collected from the precursors ranging from *m/z* 350 to 1250 for *m/z* 100–1500 for 20 ms resulting in a
184 cycle time of 3.304 s. The CE for each window was determined according to the calculation for a charge
185 +2 ion centered upon the window with variable CES according to the window.

186 **Mass spectrometry data processing**

187 A specific library of precursor masses and fragment ions was created by combining all files from the DDA
188 experiments and used for subsequent SWATH processing. Libraries were obtained using ProteinPilot™
189 software (v5.1, ABSciex®), using the following parameters: i) search against a database from SwissProt
190 composed by Homo Sapiens (released in March 2019), and MBP-GFP (15) and horse ferritin light and
191 heavy chains sequences ii) acrylamide or iodoacetamide alkylated cysteines, for whole serum or HMW
192 respectively, as fixed modification; iii) trypsin as digestion enzyme and iv) urea denaturation as a special
193 factor in the case of the HMW samples. An independent False Discovery Rate (FDR) analysis using the
194 target-decoy approach provided with Protein Pilot software was used to assess the quality of the
195 identifications, and positive identifications were considered when identified proteins and peptides
196 reached a 5% local FDR (17, 18).

197 Data processing was performed using the SWATH™ processing plug-in for PeakView™ (v2.0.01, AB
198 Sciex®) (19). After adjustment of retention time using a combination of IS and endogenous peptides, up
199 to 15 peptides, with up to 5 fragments each, were chosen per protein, and quantitation was attempted
200 for all proteins in the library file identified from ProteinPilot™ searches.

201 Protein levels were estimated based on peptides that met the 1% FDR threshold with at least 3
202 transitions in at least six samples in a group, and the peak areas of the target fragment ions of those
203 peptides were extracted across the experiment using an extracted-ion chromatogram (XIC) window of 5
204 minutes with 100 ppm XIC width. Protein levels were estimated by summing all the transitions from all
205 the peptides for a given protein (an adaptation of (20) and further normalized to the levels of the IS
206 (15)).

207 **Statistical analysis and biological interpretation**

208 Pearson's Chi-squared Test for Count Data was performed in R version 4.2.1, using the chisq.test
209 function available in the native stats package in R to determine if there were significant differences in
210 the gender proportion of the groups within the studied cohort.

211 To assess the variation of the serum proteins (either Whole serum or the HMW fraction of the serum)
212 among the three groups, a Kruskal–Wallis H test was followed by the Dunn's Test for pairwise

213 comparison. Dunn's p-values were corrected using the Benjamini-Hochberg FDR adjustment, and
214 statistical significance was considered for p-values below 0.05.

215 Stepwise Linear Discriminant Analysis (LDA) was performed to select the proteins responsible for the
216 best separation of the groups being studied. LDA was performed using IBM® SPSS® Statistics Version 22
217 (Trial). LDA was attempted considering the proteins only altered at the Whole Serum or HMW Serum,
218 and for the combination of both results. The evaluation of the models obtained from each analysis was
219 performed by comparison of the Receiver operating characteristic (ROC) curves obtained using each
220 model. A comparison of the ROC curves was performed using MedCalc Statistical Software version
221 20.106 (MedCalc Software Ltd;(21); Trial). The Delong et al. (1988) (22) method was used for the
222 calculation of the Standard Error (SE) of the Area Under the Curve (AUC) and of the difference between
223 two AUCs, and the Confidence Interval (CI) for the AUCs were calculated using the exact Binomial
224 Confidence Intervals which are calculated as the following AUC ± 1.96 SE.

225 Violin plots were used to present the distribution of the individual protein levels among each condition,
226 and Pearson's correlation analysis was performed to evaluate the similarity between the profiles of the
227 proteins highlighted in the study. Violin plots were generated using GraphPad Prism 8.0.1 (Trial) and the
228 Pearson's correlation was performed using Morpheus software (23). Heatmap and hierarchical
229 clustering analyses were computed using PermutMatrix version 1.9.3 (24, 25) using the Euclidean
230 distance and McQuitty's criteria.

231 Physical protein-protein interactions between the highlighted analytes were predicted by GeneMANIA
232 webserver (Gene Function Prediction using a Multiple Association Network Integration Algorithm; (26,
233 27) together with a gene ontology (GO) analysis of the formed network. In addition to the proteins
234 imported from this study, 28 additional related genes were allowed to create the interaction network
235 using equal weighting by network. An additional GO enrichment analysis considering the term
236 "biological process" was also performed. On the other hand, functional protein association networks
237 were evaluated using the Search Tool for Retrieval of Interacting Genes/Proteins (STRING) version 11.5
238 (28) with a medium confidence of 0.4 (29).

239 Pathway enrichment analyses were performed using the FunRich software (version 3.1.3) (30),
240 considering two different databases: the FunRich or the Reactome database. In both instances, a
241 statistical analysis employing a hypergeometric test was conducted, using the FunRich human genome
242 database as the background. Enriched pathways were considered for a non-corrected or a Bonferroni-
243 corrected p-value below 0.05 for Funrich or Reactome database, respectively.

244 ## Results

245 ### High molecular weight fractionation as a reproducible method for biomarker discovery

246 To explore the potential of HMW fractionation in peripheral biomarker research, serum samples
247 underwent either ultrafiltration using a 300 kDa MWCO filter followed by protein precipitation of the
248 retentate (referred to as HMW serum), before protein digestion and MS analysis, or were directly
249 analyzed (whole serum) (see Figure 1). In the proposed pipeline, the HMW fractionation was performed
250 under non-denaturing conditions, such that the filter would retain native HMW protein complexes and
251 large molecular structures.

252

253 **Figure 1:** Pipeline of sample preparation, data acquisition and data analysis.

254 As previously reported, employing an appropriate IS is crucial for delineating effective proteome
255 changes among different groups (12). Given the nature of the fractionation proposed in this study, an
256 ideal IS for this procedure would be a HMW protein that remains retained by the filter and bears no
257 similarity to other human proteins. In this context, equine globular protein Ferritin (~440 kDa size)
258 emerged as a suitable IS for several reasons: it lacks similarity with any other protein from the human
259 proteome (Additional File 1: Supplementary Figure 1a), the peptides monitored in the SWATH-MS
260 analysis are easily distinguishable from the matrix (the human serum proteome; Additional File 1:
261 Supplementary Figure 1b), and it exhibits a coefficient of variation similar to the one obtained by the
262 MBP-GFP used in the unfractionated analysis and previously characterized (12) (Additional File 1:
263 Supplementary Figure 1c). Additionally, the overall reproducibility of the fractionation was also
264 inspected. Similarly, to what was observed for the IS (Additional File 1: Supplementary Figure 1c), the
265 overall coefficient of variation of the proteins quantified using technical replicates (Additional File 1:
266 Supplementary Figure 1d) revealed that this procedure did not induce an appreciable increase in the
267 variability of the quantification when compared with the conventional protocol (unfractionated
268 samples). Moreover, the variation caused by the sample processing steps may be reverted by the
269 normalization of the values to the IS since the coefficient of variation of the IS is similar to the one

270 observed for the majority of the proteins, indicating that the selected IS is a good predictor of the
271 alterations induced by the method.

272 **High molecular weight fractionation increases the detection of proteomic alterations in NDs**

273 As proof of concept, this procedure was applied to serum samples of a cohort comprised of 3 different
274 groups: AD (n = 22), PD (n = 24), and CT (n = 12). No statistically significant differences were found in the
275 gender distribution between the three groups; however, differences were observed concerning age
276 distribution, with PD individuals being slightly younger, on average, than both other groups (Table 1).

277 Patients with neurodegenerative diseases, both AD and PD, were selected for this study. These
278 conditions are frequently associated with the development of abnormal protein complexes and protein
279 aggregation. Hence, they offer a fitting context to evaluate the fractionation approach's effectiveness in
280 exploring potentially altered protein interactions—an aspect frequently neglected in conventional
281 proteomics analyses.

282 **Table 1.** Study population distribution across age and sex.

	AD (n = 22)	PD (n = 24)	CT (n = 12)	p-value				
				CT vs. Diseases	CT vs. AD vs. PD	AD vs. PD	CT vs. PD	CT vs. AD
Male (n)	9	11	3	0.197*	-	0.643*	0.148*	0.262*
Female (n)	13	13	9					
Age (mean ± SD)	68.4 ± 8.2	60.3 ± 10.4	67.5 ± 7.2	-	0.014$	0.009#	0.033#	0.396#

283 * Determined by χ^2 test according to each group's male/female proportions. $ Determined by Kruskal-Wallis rank
284 sum test to compare age between all groups. # Determined by Dunn's test (Benjamini-Hochberg correction) to
285 compare age between group pairs. Diseases refer to AD and PD grouped together.

286 A total of 203 and 186 proteins were quantified in whole serum and HMW serum, respectively (Figure
287 2a, solid lines; Additional File 2: Supplementary Tables 1 and 2 for detailed information). A large overlap
288 was observed between both sample preparation procedures (168 proteins were shared, which
289 corresponds to more than 70% of all the quantified proteins). Additionally, quantification in the whole
290 serum of the proteins identified in the HMW serum library did not lead to a discernible increase in
291 proteome coverage (Figure 2a, dashed line; Additional File 2: Supplementary Table 3). Altogether, these
292 results indicate that there are no major differences in terms of the proteins being quantified in the two
293 approaches, revealing that the main aim of the HMW fractionation presented in this work –
294 fractionation under non-denaturing condition – is not the overall improvement of the proteome
295 coverage but the possibility of interrogating the samples considering protein
296 interactions/macromolecular organization.

297

298 **Figure 2 – Comparative differential proteomic analysis of whole and HMW serum of AD and PD**
299 **patients. (a)** Venn diagram comparing the number of quantified proteins in each sample type using
300 sample-specific libraries (solid lines; Additional File 2: Supplementary Tables 1-2). In addition,

301 quantification in whole serum was also performed for the proteins identified in the HMW-specific library
302 (dashed line; Serum&HMWLib condition; Additional File 2: Supplementary Table 3) to evaluate the
303 possible use of HMW fractionation as a tool to improve the proteome coverage of serum samples. A
304 total of 224 proteins were quantified in the serum samples using the three strategies referred above;
305 from those, 162 proteins were commonly quantified independently of the strategy, corresponding to
306 nearly three-quarters of all the quantified proteins (72.3%). Only three new proteins were quantified in
307 whole serum using the HMW-specific library. **(b)** Venn diagram comparing the total number of proteins
308 considered altered among the three experimental groups using the two different serum-processing
309 strategies used in this work (Additional File 1: Supplementary Figure 2 and Additional File 2:
310 Supplementary Tables 1-2). A total of 69 proteins were considered altered among the three
311 experimental groups; of those, only 11 proteins (the respective gene names are indicated) were
312 consistently considered altered independently of the strategy used. **(c)** Comparison of the levels of the
313 11 proteins commonly considered altered in both whole serum and HMW-fractionated serum. The
314 proteins were arranged considering the group comparison where the statistical differences were
315 observed (Additional File 1: Supplementary Figure 3), and the alterations were presented as the median
316 fold change observed in each sample type. Proteins considered altered in more than one group are
317 indicated in italic and with a grey shadow. Only one protein, the beta-2-glycoprotein 1 (indicated in
318 bold), presented a divergent tendency when considering its values in the whole serum versus after the
319 HMW fractionation of the samples. # - non-statistically significant difference.

320 This was further confirmed by the fact that only 14.7% of all the proteins considered altered in this study
321 (11 out of 69 proteins) were consistently altered in the fractionated and unfractionated samples (Figure
322 2b; Additional File 2: Supplementary Tables 1-2). Moreover, taking into consideration the changes of
323 those 11 commonly altered proteins, it is possible to observe that all proteins, except for the protein
324 beta-2-glycoprotein 1 (Figure 2c, bold), presented the same tendency in both fractionated and
325 unfractionated samples (Figure 2c). These results, in combination with the previous observations,
326 demonstrate that, although the two approaches quantified the same set of proteins, each method
327 interrogated the samples in a particular context, resulting in the identification of a different set of
328 altered proteins and the possibility to identify different regulatory mechanisms: while the direct analysis

329 of the serum mainly represents the alteration at the protein level, the HMW fractionation under non-
330 denaturing conditions may allow the evaluation of the physical interaction of the proteins.

331 These results are further supported by the analysis of the MW distribution of the proteins being studied,
332 which reveals a similar profile between both approaches (Additional File 1: Supplementary Figure 4a, 4b,
333 and 4c), with most of the proteins detected in HMW serum presenting a MW below 150 kDa. Moreover,
334 a similar distribution is observed for the proteins altered exclusively in the HMW approach (Additional
335 File 1: Supplementary Figure 4d), indicating that this strategy is not biased towards only the HMW
336 proteins and supporting the idea that those proteins altered in this fraction may correspond to proteins
337 being organized into different complexes.

338 **High molecular weight fractionation revealed differences in the macromolecular organization of the**
339 **serum proteome**

340 To test the hypothesis that the HMW approach is capable of evaluating the re-organization of protein
341 complexes, the nature of the 28 proteins altered exclusively in HMW serum was evaluated. This analysis
342 revealed that most of those proteins had been described to interact physically either with each other or
343 with other proteins (Figure 3a). Upon immediate observation of the GeneMania network, which
344 primarily evaluates the interactions between the proteins under study (Additional File 2: Supplementary
345 Table 4), it becomes apparent that the majority of the proteins participate in established physical
346 interactions. Moreover, it can be observed that these proteins form a large and interconnected network
347 comprising 20 of the 28 altered proteins centered around the interactions between the apolipoproteins
348 and lecithin-cholesterol acyltransferase (encoded by the *LCAT* gene). Although not participating in any
349 known interactions with another protein from the 28 altered proteins, the proteins Glutathione
350 peroxidase 3 (*GPX3*), Pigment epithelium-derived factor (*SERPINF1*), Thyroxine-binding globulin
351 (*SERPINA7*), and Alpha-1B-glycoprotein (*A1BG*) are also known to establish physical interactions
352 including with the proteins identified in this analysis. Only four of the 28 altered proteins, namely SRR1-
353 like protein (*SRRD*), carnosine dipeptidase 1 (*CNDP1*), peptidoglycan recognition protein 2 (*PGLYRP2*),
354 and serum amyloid A-4 protein (*SAA4*), were found to have no disclosed interactions in this particular
355 analysis. However, interactors for those proteins have already been pointed out in some screening

356 assays, as confirmed in BioGRID (Biological General Repository for Interaction Datasets, Additional File 2:
357 Supplementary Table 5). Furthermore, as revealed by the functional analysis, several of these 28
358 proteins are involved in the formation of complexes with lipids and platelet components (Additional File
359 2: Supplementary Table 6), indicating that those proteins can form complexes not only via the
360 interaction with other proteins but also with other molecules, and thus be organized in large complexes.
361 This involvement in the potential formation of macromolecular complexes is even more evident when
362 the functional pathways enriched in each of the two lists of proteins (30 and 28 altered proteins
363 exclusively in the whole serum or HMW serum, respectively) are directly compared (Figure 3b). This
364 comparison highlights the fact that all the pathways that are either only, or at least more, enriched in
365 the HMW dataset in comparison to the whole serum dataset (pathways indicated in bold) are related to
366 the formation/regulation of large complexes/macrostructures, namely amyloids, fibrin clot formation
367 and dissolution pathways and lipoprotein-related metabolism. On the other hand, the pathways that are
368 particularly enriched or unique in the whole serum dataset are mainly related to transcription factor
369 networks (Additional File 2: Supplementary Table 7).

370

371 **Figure 3 – Characterization of the proteins exclusively altered in whole serum or HMW serum. (a)**
372 GeneMania Network of the 28 proteins altered only at the HMW serum sample (listed in larger circles).
373 The analysis was performed with network weighting equal by network, allowing a maximum of 28 extra
374 resultant genes (non-listed small circles). The seven most enriched GeneMania Functions were
375 highlighted in the network (color code; complete results in Additional File 2: Supplementary Table 4).
376 Only protein-protein physical interactions (red edges) were considered in this analysis, demonstrating
377 that most of these 28 altered proteins have known interactors and can be involved in the formation of
378 large protein-protein complexes. **(b)** FunRich Biological Pathways enriched in the whole serum (30
379 proteins; Additional File 2: Supplementary Table 5) and HMW serum (28 proteins; Additional File 2:
380 Supplementary Table 6) proteomes. All GO analyses considered a $p < 0.05$. Pathways uniquely enriched
381 at the HMW serum or particularly enriched in this type of sample when compared to the whole serum
382 are indicated in bold.

383 **Evaluation of the potential of this combined strategy for biomarker discovery**

384 The previous set of results demonstrates that both approaches can provide complementary information.
385 In line with this evidence, the potential to use this combined strategy for biomarker discovery was also
386 evaluated. In general, both approaches result in nearly 40 proteins altered in at least one pair of
387 comparisons (Figure 4a-b; Additional File 1: Supplementary Figure 3 for details regarding each pair of
388 comparisons), with a tendency to have more proteins altered in the comparisons involving the AD group
389 (at least 20 proteins were altered compared to CT against a maximum of 14 altered proteins in PD vs.
390 CT, Additional File 1: Supplementary Figure 2a-b) and only a small subset of proteins altered in only one
391 comparison (15/41 in the whole serum and 11/39 in HMW serum, Figure 4a and 4b, respectively).
392 Besides those similarities, different profiles of altered proteins were observed depending on the
393 approach used. Hence, it can also be highlighted that while the whole serum strategy (Figure 4a) mainly
394 found proteins altered between the two disease groups (39 proteins in AD vs. PD compared to 20 and 12
395 proteins in AD vs. CT and PD vs. CT, respectively), the HMW approach (Figure 4b) captured more
396 differences between AD and CT samples (36 out of the 39 altered proteins). Due to this
397 complementarity, the combination of results from both approaches resulted in a more comprehensive
398 profile (Additional File 1: Supplementary Figure 2a-c), with a general increase in the number of altered
399 proteins per group (total of 69 altered proteins, Figure 4c). This improvement is particularly evident in
400 the case of proteins altered between PD and CT samples, for which only one protein was considered
401 commonly altered in the two approaches (Figure 2c and Additional File 1: Supplementary Figure 2b),
402 thus resulting in the duplication of the list of proteins with the potential to serve as biomarkers for PD
403 versus CT individuals. Common to all mapped profiles was the low number of proteins altered between
404 all three groups (4, 1, and 6 for Whole serum, HMW serum and the combination of both, Figure 4a-c,
405 respectively) and the absence of proteins altered exclusively between PD and CT samples.

406

407 **Figure 4 – Identification of potential circulating biomarkers of AD and PD. (a-c)** Venn diagrams
408 representing the distribution of the altered proteins among the different comparisons (AD vs. CT; PD vs.
409 CT; AD vs. PD) considering the whole serum, HMW serum and the combination of the two (Whole +

410 HMW serum) types of samples, respectively. **(d-f)** LDA using all altered proteins per sample type or the
411 combination of the two. The number of proteins used in each model is indicated above the graphic, and
412 for each model it is indicated their specificity (percentage of healthy individuals correctly identified;
413 indicated in black) and the sensitivity per disease condition (percentage of AD or PD patients correctly
414 identified; indicated in red and blue, respectively). Specificity and sensitivity values were also
415 summarized in Additional File 2: Supplementary Table 7, and the generated LDA discriminant functions
416 and their respective statistical confidence were summarized in Table 2. **(g-h)** Comparative ROC curves of
417 the discriminant functions generated using all altered proteins per sample type or a combination of the
418 two. An independent evaluation was performed for each disease group being studied. The AUC of the
419 ROC curves, their 95% CI and the pairwise comparisons are summarized in **(i)**. CI was calculated as
420 follows AUC ± 1.96 SE. n.s., non-significant alterations. * and # indicate a $p < 0.05$ for statistically
421 significant differences in comparison to the Whole Serum or HMW+Whole Serum in comparison to
422 HMW Serum, respectively, using the method of Delong et al. (1988) (22).

423 To further confirm the biomarker potential of the altered proteins from the three strategies presented
424 above, they were used as input to build discriminant models that could differentiate between the
425 studied groups (Figure 4d-f). From each dataset, candidates whose combination resulted in the best
426 possible discriminant model were automatically selected (detailed information regarding the methods in
427 Table 2), resulting in three distinct and statistically valid models (all with $p < 0.0032$) capable of
428 discriminating the three groups being studied. The whole serum dataset resulted in a reasonable model
429 composed of 4 proteins (Figure 4d), with a median sensitivity (the capacity to classify the individuals
430 from each disease group correctly) of 86.95% (sensitivity and specificity are summarized in Additional
431 File 1: Supplementary Table 8). On the other hand, the model created with six proteins from the HMW
432 approach (Figure 4e) had lower performance, with a median sensitivity of only 80.3% (corresponding to
433 83.3% predicting capacity for PD samples and 77.3% for AD samples). Moreover, neither of the models
434 was particularly good in the classification of CT samples, resulting in a specificity of only 66.7% and 75%
435 in the whole serum and HMW serum models, respectively. Remarkably, the combined model (created
436 from the dataset containing the altered proteins from both approaches - Figure 4f) clearly outperformed
437 the two models based only on proteins from a single approach. For this combined model, 10 proteins

438 were selected and integrated, creating a discriminant model capable of correctly classifying more than
439 96% of all tested samples (93% in a cross-validation test; Table 2). This included the correct classification
440 of 100% of samples from the PD group (Figure 4f), which encompassed samples from younger patients
441 compared to the other studied groups (Table 1). However, it was confirmed that this age difference did
442 not interfere with the classification of samples when employing the discriminant model since: i) age by
443 itself did not yield good classification performance (Additional File 1: Supplementary Figure 5) and ii)
444 none of the 10 proteins included in the combined model were strongly correlated with age (Additional
445 File 1: Supplementary Figure 6). Altogether, this combined method presented a median sensitivity of
446 97.75% and a specificity of 91.7%.

447 The diagnostic capacity of these models was further assessed by ROC curves, which measured their
448 ability to accurately classify AD and PD patients from among all other samples (Figure 4g-i). This analysis
449 confirmed that the best model is the one created with the combination of proteins from both
450 approaches and that, in general, the model using only proteins from the whole serum approach is better
451 than the model from the HMW approach. The respective statistics (Figure 4i) further support that the
452 whole serum model performed better than the HMW serum model but without statistically significant
453 differences between the two ROC curves. Additionally, the statistical analysis also confirmed that the
454 combined model (AUC = 0.999 for the classification of AD and PD patients) is the best model and that it
455 performed significantly better ($p < 0.05$) than both other models for PD classification (HMW serum, AUC
456 = 0.888; whole serum, AUC = 0.960) and better than the HMW serum model (AUC = 0.919) in the case of
457 AD classification. The robustness of the combined model is further evidenced by the confidence interval
458 (CI) of the AUC, which has a lower limit above 0.93 for both diseases, in contrast with the values
459 achieved for the other two methods, whose lower limits are all below 0.9.

460 **Table 2.** Linear Discriminant models, respective statistical analysis and classification results.

	Gene Name	Protein name	MW (KDa)	Whole Serum Dis 1	Whole Serum Dis 2	HMW serum Dis 1	HMW serum Dis 2	Whole + HMW serum Dis 1	Whole + HMW serum Dis 2
#	***FOXM1***	**Forkhead box protein M1**	**84.283**	---	---	---	---	**245.36**	**-10.93**
#	*PROC*	Vitamin K-dependent protein C	52.071	-1133.77	1212.34	---	---	-1557.39	623.28
#	*HBB*	Hemoglobin subunit beta (Beta-globin)	15.998	1.49	0.58	-0.06	-0.13	0.42	-1.50
#	*APOA1*	Apolipoprotein A1 (Apo-AI)	30.778	3.63	0.53	---	---	-0.16	-3.08
#	***IGLV3-19***	**Immunoglobulin lambda variable 3-19**	**12.042**	---	---	---	---	**62.89**	**52.70**
§	*SRRD*	SRR1-like protein	38.573	---	---	20.37	7.55	16.69	11.52
§	*APOC1*	Apolipoprotein C1 (Apo-CI)	9.332	---	---	-9.74	19.21	-15.77	1.33
§	*APOE*	Apolipoprotein E (Apo-E)	36.154	---	---	1.46	-0.42	0.84	0.53
§	***SERPINF1***	**Pigment epithelium-derived factor (PEDF)**	**46.312**	---	---	---	---	**6.85**	**2.63**
§	*KRT9*	Keratin, type I cytoskeletal 9	62.064	---	---	-8.80	5.05	-12.73	-4.91
	PPBP	**Platelet basic protein (PBP)**	**13.894**	---	---	**8.89**	**-7.88**	---	---
	TF	**Serotransferrin (Transferrin)**	**77.050**	**-0.99**	**-1.66**	---	---	---	---
		(Constant)		2.11	-0.81	-1.11	-2.82	3.34	-1.10
	Statistics (Wilks' Lambda, Chi-square and p-value)		**λ=**	0.253	0.773	0.242	0.629	0.058	0.292
			χ2=	73.473	13.473	74.458	24.361	143.675	62.244
			p<	9.97×10^{-13}	3.23×10^{-03}	4.65×10^{-11}	1.85×10^{-04}	1.01×10^{-20}	4.94×10^{-10}
	Overall classification results (% of cases correctly classified)		**Original**	82.8		79.3		96.6	
			Cross-validation	81.0		72.4		93.1	

461 # selected from the data from the whole serum approach for the Whole + HMW serum model; § selected from the data from the HMW serum approach for the Whole + HMW serum model;

462 Dis – discriminant function; Note that proteins are sorted by order of inclusion into the Whole + HMW serum discriminant model. Proteins exclusive to one of the models appear in bold.

463 By looking at the proteins selected to build the different methods (Table 2), it was observed that the
464 combined method is not the simple combination of the proteins previously selected from each of the
465 individual methods. The combined model is built by the combination of 10 proteins, five from each
466 dataset, including three [forkhead box protein M1 (*FOXM1*), immunoglobulin lambda variable 3-19
467 (*IGLV3-19*) and pigment epithelium-derived factor (*SERPINF1*)] that were not selected on the database-
468 specific models. On the other hand, some previously selected proteins [serotransferrin (*TF*) and platelet
469 basic protein (*PPBP*)] were not included in the combined model. Finally, the Hemoglobin subunit beta
470 (*HBB*) was selected in both approach-specific models, although only data from the whole serum dataset
471 was used in the combined model. These results demonstrate that the increase in the initial amount of
472 data provided for the discriminant analysis has an important impact on the generated model by making
473 it possible to test different combinations of proteins and, thus, allowing for the identification of better
474 combinations than those highlighted in the analysis of individual datasets. Interestingly, all ten proteins
475 selected in the combined model have a MW below 90 kDa (Table 2). This finding confirms that all the
476 proteins selected from the HMW approach have a MW below the theoretical cut-off of the filters used
477 for fractionation. This observation supports the hypothesis that this approach might effectively assess
478 the remodeling of molecular complexes. By plotting the individual values of each of the ten proteins
479 selected in the combined model (Figure 5a), it is possible to observe that, as expected, those values
480 present some variation characteristic of the individuality of each patient. Nevertheless, considering that
481 the model was able to correctly classify more than 90% of all the patients (Figure 4f), it is possible to
482 infer that the combinations performed in the model could diminish the impact of the biological
483 variability, proving that the combination of different markers can overcome their individual weaknesses.
484 The analysis of these results immediately reveals that i) only three proteins from the model (the
485 proteins encoded by the genes *FOXM1, HBB,* and *SRRD*) are significantly altered between all three
486 groups and ii) only one protein, the apolipoprotein C1 (Apo-CI, encoded by the *APOC1* gene), is altered
487 between a single comparison, in this case between AD and PD which may indicate that this protein may
488 have a particularly important role in this model for distinguishing AD from PD patients. Among the
489 remaining 6 proteins: i) three, apolipoprotein E, pigment epithelium-derived factor and KRT9, are
490 altered between both disease groups and control sample (all three found in the HMW fraction); ii) two,
491 apolipoprotein A1 and immunoglobulin lambda variable 3-19, are altered in AD in comparison to both

492 PD and CT, and one, the Vitamin K-dependent protein C (encoded by the PROC gene), is altered in PD
493 patients in comparison to the other two groups. Moreover, it is noteworthy that while there was a
494 tendency to incorporate proteins that were increased in AD compared to CT from the whole serum
495 approach (three out of the five proteins from the whole serum model, encoded by the genes *FOXM1*,
496 *HBB*, and *APOA1*), the opposite trend was observed in the case of proteins from the HMW approach.
497 Specifically, three out of the five proteins (the proteins encoded by the genes *SRRD*, *APOE*, and
498 *SERPINF1*) were found to be decreased in the AD vs. CT comparison. On the contrary, for the PD vs. CT
499 comparison, there were no major differences in terms of tendencies when considering the proteins
500 captured in the whole serum or the HMW serum.

501 Finally, all proteins from the whole serum dataset, in addition to SRR1-like protein (encoded by the
502 *SRRD* gene) and Apo-CI from the HMW dataset, were significantly altered between both disease groups.
503 From these, three proteins [the protein Forkhead box protein M1 (encoded by the *FOXM1* gene),
504 hemoglobin subunit beta (encoded by *HBB* gene), and apolipoprotein A1 (Apo-AI, encoded by the
505 *APOA1* gene)] are less abundant in PD samples than in AD samples, while the remaining four are
506 increased.

507

508 **Figure 5 – Characterization of the protein panel selected by the combined LDA model. (a)** Violin plots
509 representing the protein level distribution of the ten proteins from the model. The dashed lines indicate
510 the first, second (median) and third quartiles. *, **, and *** indicate a $p < 0.05$, $p<0.01$, and $p<0.001$
511 for statistically significant differences. * denotes the comparison to control and # the differences
512 between disease groups. Statistical analysis was performed using the Kruskal–Wallis H test followed by
513 the Dunn's Test for pairwise comparison. **(b)** Pearson's correlation analysis between the overall
514 regulation profile of the proteins included in the model. **(c)** Heatmap and hierarchical clustering analysis
515 of the proteins from the model. Clustering was performed for both proteins and individuals. Three
516 different clusters (Cluster PD, CT and AD) containing the large majority of the individuals from a given
517 group can be highlighted from the analysis. The average profile of each cluster is indicated on the right
518 and can be considered as the profile of expression of those proteins within the groups considered in this

519 study. **(d)** Interaction network of these proteins carried out with STRING with a medium confidence (0.4)
520 score. The color of the edges indicates the type of evidence that supports the interaction, while the
521 color of the nodes represents the categorization of the proteins considering UniProt Keywords. The
522 calculated PPI enrichment p-value is 2.07e-05. Three clusters (Cluster 1 to 3) can be identified within the
523 network, with the dashed edges indicating the separation between clusters. Cluster 1 corresponds to
524 proteins whose interactions are experimentally confirmed, cluster 2 is composed of theoretically related
525 proteins, and cluster 3 corresponds to non-related proteins. **(e)** Reactome pathways enrichment analysis
526 using the proteins from the model. The red line indicates Bonferroni's corrected p-value with the
527 corrected $p < 0.05$, meaning a significant enrichment. The grey dashed line indicates the reference line
528 ($p = 0.05$).

529 The correlation analysis of the protein abundances among groups confirmed that, in general, there is no
530 particularly evident correlation between the profiles and the magnitude of regulation of these proteins
531 (Figure 5b). There were, however, some observed exceptions, including a strong positive correlation
532 between the proteins encoded by the genes *APOA1* and *FOXM1* (r = 0.8) and, to a lesser extent, the
533 proteins encoded by *APOC1, APOE and SERPINF1* (r = 0.5-0.6). Interestingly, the proteins showing a
534 positive correlation originated from the same approach, the gene products of *APOA1* and *FOXM1* were
535 both highlighted in the whole serum approach, suggesting that the overall levels of these two proteins
536 were similarly altered. Meanwhile, the products of the *APOC1, APOE,* and *SERPINF1* genes were
537 identified as altered in the HMW fractionation strategy, which may indicate that these proteins might be
538 part of the same complex and thus regulated in a similar manner. No remarkable negative correlations
539 were found, with the strongest correlation observed between the proteins encoded by the *APOA1* and
540 *SRRD* genes, which indicates that none of the proteins in the model present a completely opposite
541 regulation profile. Additionally, an unsupervised clustering analysis using these ten proteins (Figure 5c)
542 confirmed their capacity to partially distinguish the three groups being studied, revealing that, besides
543 the existence of individual variability, it was possible to identify three independent clusters composed
544 exclusively or mainly of samples from one of the three groups. This analysis also demonstrates that this
545 set of proteins is particularly efficient in isolating the AD patients from the remaining individuals from
546 the study: the AD cluster was composed exclusively of AD patients, and only 6 out of the 22 AD patients

547 were not included in this cluster. On the other hand, a slightly lower separation capacity was observed
548 for both PD and CT samples. These two clusters contained few samples that did not belong to their
549 respective groups, resulting in a higher percentage of individuals not properly grouped (10 out of 24 and
550 4 out of 12 samples for PD and CT, respectively). The discrepancies observed between the clustering
551 analysis and the discriminant model results, where the latter correctly classified over 90% of the
552 samples, can be attributed to the fact that the clustering analysis relied solely on the individual protein
553 distribution profiles across the samples. In contrast, the discriminant analysis employed equations with
554 different weightings for each protein, resulting in a single model that effectively reduces the intragroup
555 variability while promoting a better separation between the analyzed groups. Despite that, the
556 clustering analysis remains an important approach for understanding how the proteins are modulated
557 within the samples. Thus, from the three different clusters highlighted in the analysis, it was possible to
558 infer the median protein abundance profile of these proteins among the three groups. For instance, the
559 gene products of *SERPINF1, APOE* and *APOC1* tend to be less abundant in both disease groups compared
560 to CT samples. Furthermore, some proteins are more abundant in each disease group, namely the gene
561 products of *PROC* and *KRT9* in PD samples and the gene products of *HBB, APOA1* and *FOXM1* in AD
562 samples. Another disease-specific observation was the smaller amount of immunoglobulin lambda
563 variable 3-19 (*IGLV3-19*) in AD samples compared to both other groups. Overall, these tendencies
564 characterize the unique profiles determined for each disease group, which may be a precursor to a
565 potential future biomarker panel that could be more informative than the analysis based on any single
566 protein.

567 Finally, STRING analysis (Figure 5d and Additional File 2: Supplementary Table 9) revealed that these ten
568 proteins have more interactions among themselves than what would be expected for a random set of
569 proteins of the same size and degree of distribution, indicating that this set of proteins is, at least
570 partially, biologically connected (PPI enrichment $p = 2.07\times10^{-5}$). This result may be mainly due to the
571 strong network involving apolipoproteins and Hemoglobin subunit beta (cluster 1). Again, two out of the
572 ten proteins selected for the discriminant method revealed to be associated with high-density
573 lipoproteins (HDL) and chylomicron (ultra-low-density lipoproteins particles) remodeling and assembly
574 (Figure 5e and Additional File 2: Supplementary Table 10), highlighting the potential importance of these

575 mechanisms in the neurodegenerative process, and confirming that the proteins related with these
576 mechanisms could be good biomarker candidates for their diagnosis.

577 Given the central role that apolipoproteins appear to play in this model, a discriminant analysis was
578 performed using data from ten altered proteins involved in apolipoprotein-related mechanisms to
579 investigate if the diagnostic model could be limited to this set of functionally related proteins (Additional
580 File 1: Supplementary Figure 7). However, the generated model exhibited lower diagnostic capacity
581 compared to the combined approach, with only 82.75% of the samples being correctly classified. The
582 model demonstrated a specificity of 66.7%, and a sensitivity of 86.4% and 87.5% for AD and PD,
583 respectively, yielding ROC curves with AUCs equal to or below 0.955. Thus, besides the importance of
584 apolipoproteins, the results from these proteins alone are not enough to distinguish the three groups,
585 emphasizing the importance of having diagnostic models based on several complementary candidates
586 instead of a single or just a few candidates. Nonetheless, the identification of this robust core of
587 functionally related proteins underscores the significance of the combined approach for identifying new
588 potential biomarkers. For instance, while the dysregulation of Apo-C1 and Apolipoprotein E (Apo-E,
589 encoded by the *APOE* gene) was discovered using the HMW fractionation approach, the dysregulation of
590 Apo-AI was identified using the whole serum approach.

591 ## Discussion

592 The present study presents a proof of concept of a novel two-pronged approach to biomarker discovery
593 in complex peripheral biological fluids. More specifically, it was demonstrated that through the
594 combination of two complementary proteomics strategies, the direct analysis of whole serum and the
595 analysis of serum HMW fraction (above 300 kDa) in non-denaturing conditions, another level of
596 proteome characterization of the samples could be achieved. This resulted in more robust diagnostic
597 models and insights into disease mechanisms. In this sense, when applied to serum samples from a
598 cohort of control individuals and individuals afflicted by neurodegenerative diseases, this strategy
599 allowed for a strong discriminant model to be built, able to distinguish all studied groups more
600 effectively than the models generated from a single proteomics analysis. The most noticeable findings
601 from this model showed that several, otherwise overlooked, proteins may yet serve as potential
602 biomarkers of disease, in this case, AD and PD, particularly when analyzed together in a model created
603 using the two different approaches. Thus, these results confirm the importance of having a panel of
604 potential candidates rather than a single protein biomarker. Furthermore, they also demonstrate that
605 the biomarker discovery field will benefit from combining data from the sample obtained through
606 different sample processing strategies. While not individually sufficient to be considered as biomarkers,
607 the significant influence of apolipoproteins, particularly Apo-AI, Apo-CI, and Apo-E, in the
608 aforementioned discriminant model, suggests a potential disease-specific dysregulation of lipoprotein
609 metabolism in AD and PD patients.

610 **High molecular weight fractionation may reveal a potentially altered macromolecular and**
611 **macromolecular-complex organization**

612 In this work, it was demonstrated that interrogating serum samples with the HMW fractionation
613 method adds an extra layer of information capable of bringing new insight into the behavior of the
614 serum proteins, particularly regarding their potential macromolecular organization. Because the
615 fractionation procedure took place under non-denaturing conditions and since aberrant protein
616 aggregation (8) is a common hallmark of both AD and PD, it was hypothesized that macromolecular

617 complexes, potentially altered between the studied groups, could be captured through the HMW
618 fractionation approach.

619 The present results confirmed this premise, as evidenced by the fact that although no variation was
620 observed in the overall serum protein captured by both strategies, proteins exclusively altered in the
621 HMW fraction accounted for 40% of the total list of altered proteins. Furthermore, with the exception of
622 one protein (Centrosome-associated protein CEP250), all proteins had a MW below 90 kDa, which is
623 considerably lower than the 300 kDa cut-off filter used. It is worth noting that 72% of proteins altered in
624 the HMW fraction did not exhibit alterations in their total levels. This supports the possibility that
625 different regulatory mechanisms of these proteins, apart from expression and degradation, are being
626 revealed and studied using this approach.

627 Moreover, the results show that most of these proteins have several reported interactors and thus may
628 be involved in the formation of large complexes. An illustration of this phenomenon is found in the
629 protein clusterin (CLU gene), also known as apolipoprotein J, which has been implicated in the
630 metabolism of aggregation-prone proteins, including those associated with NDs (31-33). Notably,
631 clusterin's interaction with Aβ42 has been demonstrated to enhance its clearance from the brain
632 through the blood-brain barrier (BBB) (31). Furthermore, clusterin has been implicated in various stages
633 of PD, potentially exerting a neuroprotective effect through its interaction with α-synuclein aggregates
634 (32). Additionally, the interaction between clusterin and α-synuclein has been detected in plasma
635 samples (33). Beyond this specific example, the generic functional analysis of altered proteins,
636 particularly those from the HMW serum strategy, suggests their close association with amyloids and clot
637 formation, which may involve large structures.

638 On the other hand, some of these proteins may instead, or additionally, be present in large biological
639 structures not composed exclusively of proteins, like exosomes or lipoproteins, which would not only
640 likewise justify their presence in this HMW serum fraction but also give further understanding of the
641 potentially altered mechanisms related to the diseases being studied. Such may be the case of the
642 proteins clusterin and serum amyloid A-4 (*SAA4* gene), which were found to be altered in serum neuron-
643 derived exosomes of AD patients (34). Additionally, exosomal clusterin was found to be altered in

644 patients at different stages of PD when compared to controls (35). Thus, although the presence of
645 exosomes in the HMW fraction was not confirmed, given the MWCO of the filters used in this work, it is
646 feasible that some of the proteins being analyzed in the HMW fraction may correspond to proteins
647 linked to the extracellular vesicles.

648 Altogether, these findings support the notion that the HMW fractionation approach can provide a new
649 level of information that may offer new insights into how proteins are organized within a given sample.

650 **Altered lipoprotein metabolism can be a peripherical marker of AD and PD**

651 The combination of the two approaches in this study led to a robust and promising potential biomarker
652 panel composed of ten proteins quantified in whole serum or HMW serum. A major finding revealed by
653 this model was the involvement of several lipoproteins in discriminating between the studied groups.
654 Among the ten proteins used in the best discriminant model, three are apolipoproteins: Apo-AI from
655 whole serum, and Apo-CI and Apo-E from HMW serum. Besides those three proteins, other altered
656 apolipoproteins were observed in this study but not included in the model, namely: i) the Apo-AII, Apo-
657 LI and clusterin highlighted in the HMW serum strategy; ii) the Apo-AIV from the whole serum; and, iii)
658 beta-2-glycoprotein 1 in both approaches. Furthermore, a lipoprotein-related enzyme, lecithin-
659 cholesterol acyltransferase, was also altered in HMW serum. This is further supported by the functional
660 enrichment analysis of the altered proteins discovered in both strategies that highlight the involvement
661 of those proteins in lipoprotein metabolism and HDL-mediated lipid transport pathways. Cumulatively,
662 all these findings point to the relevance of lipoproteins in the context of NDs and, although not
663 absolutely clear, the link between these diseases, in particularly AD, and apolipoproteins has been the
664 focus of many studies (31, 33, 36-46).

665 Apo-AI and Apo-E have an established relation to toxic species clearance from the brain in AD and PD
666 (31, 33, 37, 47-50). Additionally, regarding AD, our findings for both proteins contradict what can be
667 found in the literature (38, 43). For Apo-AI, we found an increase in abundance in AD patients as
668 opposed to the decrease reported for most studies (38). However, in another study where no significant
669 alterations in total serum Apo-AI content of AD patients were reported, further investigation revealed
670 that some proteoforms of this protein were significantly increased compared to the levels observed in

671 the controls (39). This has been suggested as a possible explanation for the different observations
672 regarding this protein in the context of AD, which might be related to the use of different detection
673 methods within different studies (38). Regarding this protein's connection to clearance mechanisms,
674 evidence suggests that for HDLs containing Apo-AI (APOA1-HDL), the structure seems to influence not
675 only the disaggregation of Aβ fibrils but also its ability to cross the BBB, with lipid-poor discoidal APOA1-
676 HDL having the best performance when compared to APOA1-HDL in other lipidation states (37).
677 Moreover, in the present study, phosphatidylcholine-sterol acyltransferase, an enzyme known to affect
678 HDL structure through lipidation of Apo-AI in plasma (45), was also found to be altered in AD patients.
679 As this enzyme participates in HDL maturation in plasma (51), this result could reflect the dysregulation
680 of lipoproteins in AD. For Apo-E, we found a decrease in abundance in AD patients as opposed to the
681 increase reported for MCI patients in a previous study (43). Isoform and lipidation status of Apo-E is also
682 crucial for the Aβ clearance, with the Apo-E4 isoform, the genetic risk factor most associated with the
683 onset of AD (31, 48), and higher lipidation having detrimental effects on the process (31, 48). Further
684 investigation using the combined approach presented in this study, particularly in the context of AD,
685 should also involve a lipid profile analysis and APOE genotyping of the participants to enable a more
686 comprehensive characterization of serum HDLs and Apo-E content, respectively.

687 Although systemic lipid abnormalities have also been implicated in PD, there are fewer findings
688 connecting it to HDL-related proteins, as compared to AD (32). Nonetheless, a previous report observed
689 significantly decreased values of Apo-AI in mild PD patients compared to healthy controls, but much like
690 what we observed for this protein, a less impactful and non-significant decrease was observed in
691 moderate/severe PD patients (52). In fact, most research indicates that Apo-AI may have a protective
692 role in PD (32) and it has been hypothesized that APOA1-HDL could take part in the efflux of α-synuclein
693 from the brain (33). Additionally, both Apo-AI and Apo-E have been reported to interact with α-
694 synuclein (33).

695 Finally, HDL size and plasma levels have been shown to be dependent on the levels of Apo-CI (53),
696 another apolipoprotein included in the best diagnostic model generated in this study. Besides that, a
697 previous study also shows that the dysregulation of this protein can lead to impaired memory processes
698 in mice (54). This suggests that the regulation of Apo-CI can be pivotal in the brain and that a systemic

699 disruption of this process could have effects detectable beyond the CNS, particularly in lipoprotein
700 metabolism, that could be observable in peripheral biofluids. Interestingly, this study found that Apo-CI
701 significantly decreased in the HMW serum fraction of AD compared to PD patients, but only a slight and
702 non-significant decrease was observed when compared to CT patients. Similarly, only a small non-
703 significant decrease in HMW serum Apo-CI was observed for controls in comparison to PD patients,
704 which is in accordance to what was already reported for whole plasma (40). Given that memory
705 impairment is a hallmark of AD and not a predominant feature among PD patients (55), these results
706 may be influenced, at least in part, by the age disparities observed between the PD group and the other
707 two groups. In fact, PD patients are, on average, younger than those in the other two groups, with
708 similar age distributions. Additionally, the results regarding Apo-CI may also be affected by individual
709 Apo-CI and Apo-E isoforms. Notably, the *APOE* and *APOC1* genes are in linkage disequilibrium (56), and
710 carriers of the *APOE(ε4)* and *APOC1(H2)* alleles have been demonstrated to have an increased risk of
711 developing AD (46). This was further confirmed in a study using human *APOE*-carrying mice, which
712 demonstrated that those animals carrying the *APOE(ε4)* allele were found to have decreased serum
713 Apo-CI content when compared to those carrying the *APOE(ε3)* allele (57). However, Apo-CI has also
714 been suggested to potentially play a modulatory role in the development of AD, with reported effects
715 on mice cognitive function independent of Apo-E expression (58). Again, these observations strengthen
716 the importance of combining these results with further characterization of the individuals, including
717 genotyping of the apolipoproteins' isoforms.

718 Although these three apolipoproteins have been linked to AD and PD, as evidenced by previously
719 mentioned studies, and their relevance for the discriminant model, their use alone or in combination
720 with other proteins associated with apolipoprotein-related mechanisms did not result in a robust
721 diagnostic model capable of effectively distinguishing between the studied groups (as shown in
722 Additional File 1: Supplementary Figure 7). This indicates that these three apolipoproteins had to be
723 combined with other seemingly unrelated proteins to be used as potential biomarkers. Further studies
724 should be directed towards elucidating this potential relationship to understand: i) the importance of
725 the identified proteins/mechanisms for the pathophysiology of the studied NDs, and ii) to which extent
726 these mechanisms are differently altered between the two diseases.

727 **Conclusion**

728 In summary, this work demonstrated that combining two complementary sample processing
729 approaches is a more effective strategy to reach potential biomarkers than a single approach. Besides
730 that, the strategies used here, which combine the analysis of the whole serum and the HMW
731 fractionation of non- denaturing serum, can also identify proteins being differentially modulated besides
732 the conventional alteration in their total levels. In this work, this new strategy was applied to a cohort of
733 NDs patients and respective CT individuals, being able to build a good predictive model capable of
734 distinguishing all the three groups studied (AD, PD and CT). This predictive model highlighted the linkage
735 of the apolipoprotein family and NDs, with three out of the ten proteins included in this model being
736 apolipoproteins. Nevertheless, further validation in a larger and independent cohort is needed to
737 confirm the robustness and reliability of the model, as well as more studies to link the alterations
738 observed and these pathologies. Controlling the lipid profile in future studies is also advised, as altered
739 lipid metabolism was a major finding of the present work. Another aspect to be further explored would
740 be the identification of protein complexes in the HMW fraction to better understand the origin of the
741 protein alterations observed.

742 Overall, the results of this study demonstrate that HMW fractionation under non-denaturing conditions
743 could be a valuable addition to routine biofluid analysis, particularly regarding the detection of changes
744 in macromolecular organization. Furthermore, this study highlights the importance of exploring the
745 involvement of apolipoproteins and lipid metabolism in greater detail within the context of NDs.

746 **List of abbreviations**

747 AD, Alzheimer's Disease; APOA1-HDL, High-Density Lipoproteins containing Apolipoprotein A1; AUC,
748 Area Under the Curve; Aβ, Amyloid-β; BBB, Blood-Brain Barrier; BioGRID, Biological General Repository
749 for Interaction Datasets; CE, Collision Energy; CES, Collision Energy Spread; CHUC, Centro Hospitalar e
750 Universitário de Coimbra; CI, Confidence Interval; CNS, Central Nervous System; CT, Healthy Controls;
751 DDA, Data-dependent Acquisition; DMSO, Dimethyl Sulfoxide; FA Formic Acid; FDR, False Discovery
752 Rate; GO, Gene Ontology; HDL, High-Density Lipoproteins; HMW, High Molecular Weight; IS, Internal
753 Standard; LDA, Linear Discriminant Analysis; MCI, Mild Cognitive Impairment; MS, Mass Spectrometry;
754 MW, Molecular Weight; MWCO, Molecular Weight Cut-Off; NDs, Neurodegenerative Diseases; PD,
755 Parkinson's Disease; ROC, Receiver Operating Curve; SE, Standard Error; STRING, Search Tool for
756 Retrieval of Interacting Genes/Proteins; XIC, Extracted Ion Chromatogram.

757 ## Declarations

758 **Ethics approval and consent to participate**

759 The study was approved by the Ethics Committee of the Faculty of Medicine of the University of
760 Coimbra (reference CE_010.2017) and the Ethics Committee of the Centro Hospitalar e Universitário de
761 Coimbra (CHUC) (reference 34 /CES-CHUC-024-18) and was conducted according to the principles stated
762 in the Declaration of Helsinki (59). Written informed consent was obtained from all participants.

763 **Consent for publication**

764 Not applicable

765 **Availability of data and materials**

766 The MS proteomics data have been deposited to the ProteomeXchange Consortium (60) via the PRIDE
767 (61) partner repository with the dataset identifier PXD034077.

768 **Competing interests**

769 The authors declare that they have no competing interests

770 **Funding**

771 The authors would like to thank the financial support of the European Regional Development Fund
772 (ERDF), through the COMPETE 2020 - Operational Programme for Competitiveness and
773 Internationalisation and Portuguese national funds via FCT – Fundação para a Ciência e a Tecnologia,
774 I.P., under projects: MEDPersyst - POCI-01-0145-FEDER-016428 (ref.: SAICTPAC/0010/2015), POCI-01-
775 0145-FEDER-30943 (ref.: PTDC/MEC-PSQ/30943/2017), PTDC/MED-NEU/27946/2017, POCI-01-0145-
776 FEDER-016795 (ref.: PTDC/NEU-SCC/7051/2014), POCI-01-0145-FEDER-029311 (ref.: PTDC/BTM-
777 TEC/29311/2017); EXPL/BTM-TEC/1407/2021, and, UIDB/04539/2020, UIDP/04539/2020,
778 UIDB&P/4950/2020 and LA/P/0058/2020, and the National Mass Spectrometry Network (RNEM) [POCI-
779 01-0145-FEDER-402-022125 Ref. ROTEIRO/0028/2013). SIA was supported by the CEEC grant
780 2021.04378.CEECIND and MR was supported by Ph.D. fellowship 2020.07749.BD.

781 **Authors' contributions**

782 SIA and BM conceived and designed the study. SIA and MR performed all the experiments, data analysis,
783 and wrote the manuscript. IB, AG, DP, CS, JP, CJ, IS, AV, AM, and MCB were involved in the selection and
784 collection of the plasma samples used in this study. MCB and BM were responsible for funding. The
785 author(s) read and approved the final manuscript.

786 **Acknowledgements**

787 Not applicable

788 **Authors' information (optional)**

789 Not applicable

790 ## Additional files

791 **Additional File 1 (.docx)** – Supplementary Figure 1: Internal standard proteins and ultrafiltration
792 reproducibility; Supplementary Figure 2: Altered proteins quantified using the whole serum dataset and
793 HMW serum dataset; Supplementary Figure 3: Volcano plots comparing all proteins quantified across
794 the three different experimental groups using the two different serum-processing strategies;
795 Supplementary Figure 4: Mass distribution of proteins identified or quantified using different
796 approaches; Supplementary Figure 5: Linear discriminant analysis using patient's age; Supplementary
797 Figure 6: Correlation between quantification of the 10 proteins included in the combined model and
798 patient age; Supplementary Figure 7: Linear discriminant analysis using 10 altered proteins associated
799 with apolipoprotein related mechanisms; Supplementary Table 8 – Summary of the specificity and
800 sensitivity of the LDA methods obtained using all the altered proteins per sample type (whole serum or
801 HMW serum) or the combination of the two (Whole + HMW serum).

802 **Additional File 2 (.xlsx)** – Supplementary Table 1 - Evaluation of the total levels of proteins at the
803 unfractionated serum (Whole Serum) of Control and Alzheimer's and Parkinson's Disease patients;
804 Supplementary Table 2 - Evaluation of the total levels of proteins at the high molecular fraction of the
805 serum (HMW Serum) of Control and Alzheimer's and Parkinson's Disease patients; Supplementary Table
806 3 - Evaluation of the total levels of proteins at the unfractionated serum (Whole Serum) of Control and
807 Alzheimer's and Parkinson's Disease patients; Supplementary Table 4 - Descriptive table of the
808 GeneMania functional enrichment analysis of the 28 proteins exclusively quantified in the HMW serum
809 samples; Supplementary Table 5 - Descriptive table of protein physical interactions reported in BioGRID
810 for the four proteins (marked in yellow) with no reported interactions according to the GeneMania
811 network (Figure 3a); Supplementary Table 6 - Descriptive table of the Funrich Biological Pathway
812 Analysis of the 30 proteins exclusively quantified in Whole serum samples; Supplementary Table 7 -
813 Descriptive table of the Funrich Biological Pathway Analysis of the 30 proteins exclusively quantified in
814 HMW serum samples; Supplementary Table 9 - Descriptive table of the String Enrichment Analysis of the
815 10 proteins used in the LDA combined model; Supplementary Table 10 - Descriptive table of the
816 Reactome Pathway enrichment analysis of the 10 proteins used in the LDA combined model.

817 **References**

818 1. Anderson NL, Anderson NG. The Human Plasma Proteome: History, Character, and Diagnostic
819 Prospects*. Molecular & Cellular Proteomics. 2002;1(11):845-67.

820 2. Antoranz A, Sakellaropoulos T, Saez-Rodriguez J, Alexopoulos LG. Mechanism-based biomarker
821 discovery. Drug Discovery Today. 2017;22(8):1209-15.

822 3. Anjo SI, Santa C, Manadas B. SWATH-MS as a tool for biomarker discovery: From basic research
823 to clinical applications. PROTEOMICS. 2017;17(3-4):1600278.

824 4. Anjo SI, Manadas B. A translational view of cells' secretome analysis - from untargeted
825 proteomics to potential circulating biomarkers. Biochimie. 2018;155:37-49.

826 5. Rosado M, Silva R, G. Bexiga M, G. Jones J, Manadas B, Anjo SI. Chapter Four - Advances in
827 biomarker detection: Alternative approaches for blood-based biomarker detection. In: Makowski GS,
828 editor. Advances in Clinical Chemistry. 92: Elsevier; 2019. p. 141-99.

829 6. Greening DW, Simpson RJ. A centrifugal ultrafiltration strategy for isolating the low-molecular
830 weight (≤25K) component of human plasma proteome. Journal of Proteomics. 2010;73(3):637-48.

831 7. Greening DW, Simpson RJ. Low-Molecular Weight Plasma Proteome Analysis Using Centrifugal
832 Ultrafiltration. In: Simpson RJ, Greening DW, editors. Serum/Plasma Proteomics: Methods and
833 Protocols. Totowa, NJ: Humana Press; 2011. p. 109-24.

834 8. Espay AJ, Vizcarra JA, Marsili L, Lang AE, Simon DK, Merola A, et al. Revisiting protein
835 aggregation as pathogenic in sporadic Parkinson and Alzheimer diseases. Neurology. 2019;92(7):329-37.

836 9. Hughes AJ, Daniel SE, Kilford L, Lees AJ. Accuracy of clinical diagnosis of idiopathic Parkinson's
837 disease: a clinico-pathological study of 100 cases. Journal of Neurology, Neurosurgery & Psychiatry.
838 1992;55(3):181-4.

839 10. American Psychiatric Association A, Association AP. Diagnostic and statistical manual of mental
840 disorders: DSM-IV: American psychiatric association Washington, DC; 1994.

841 11. McKhann GM, Knopman DS, Chertkow H, Hyman BT, Jack Jr CR, Kawas CH, et al. The diagnosis
842 of dementia due to Alzheimer's disease: Recommendations from the National Institute on Aging-
843 Alzheimer's Association workgroups on diagnostic guidelines for Alzheimer's disease. Alzheimer's &
844 dementia. 2011;7(3):263-9.

845 12. Anjo SI, Simoes I, Castanheira P, Graos M, Manadas B. Use of recombinant proteins as a simple
846 and robust normalization method for untargeted proteomics screening: exhaustive performance
847 assessment. Talanta. 2019;205:120163.
848 13. Anjo SI, Santa C, Manadas B. Short GeLC-SWATH: a fast and reliable quantitative approach for
849 proteomic screenings. Proteomics. 2015;15(4):757-62.
850 14. Santa C, Anjo SI, Manadas B. Protein precipitation of diluted samples in SDS-containing buffer
851 with acetone leads to higher protein recovery and reproducibility in comparison with TCA/acetone
852 approach. Proteomics. 2016;16(13):1847-51.
853 15. Anjo SI, Melo MN, Loureiro LR, Sabala L, Castanheira P, Grãos M, et al. oxSWATH: An integrative
854 method for a comprehensive redox-centered analysis combined with a generic differential proteomics
855 screening. Redox biology. 2019;22:101130.
856 16. Gillet LC, Navarro P, Tate S, Röst H, Selevsek N, Reiter L, et al. Targeted data extraction of the
857 MS/MS spectra generated by data-independent acquisition: a new concept for consistent and accurate
858 proteome analysis. Molecular & Cellular Proteomics. 2012;11(6).
859 17. Tang WH, Shilov IV, Seymour SL. Nonlinear fitting method for determining local false discovery
860 rates from decoy database searches. Journal of proteome research. 2008;7(9):3661-7.
861 18. Sennels L, Bukowski-Wills JC, Rappsilber J. Improved results in proteomics by use of local and
862 peptide-class specific false discovery rates. BMC Bioinformatics. 2009;10:179.
863 19. Lambert J-P, Ivosev G, Couzens AL, Larsen B, Taipale M, Lin Z-Y, et al. Mapping differential
864 interactomes by affinity purification coupled with data-independent mass spectrometry acquisition.
865 Nature methods. 2013.
866 20. Collins BC, Gillet LC, Rosenberger G, Röst HL, Vichalkovski A, Gstaiger M, et al. Quantifying
867 protein interaction dynamics by SWATH mass spectrometry: application to the 14-3-3 system. Nature
868 methods. 2013.
869 21. MedCalc. https://www.medcalc.org. Accessed 19 April 2022
870 22. DeLong ER, DeLong DM, Clarke-Pearson DL. Comparing the areas under two or more correlated
871 receiver operating characteristic curves: a nonparametric approach. Biometrics. 1988:837-45.
872 23. MORPHEUS. https://software.broadinstitute.org/morpheus/. Accessed 24 May 2022

873 24. Caraux G, Pinloche S. PermutMatrix: a graphical environment to arrange gene expression
874 profiles in optimal linear order. Bioinformatics. 2005;21(7):1280-1.
875 25. PermutMatrix. http://www.atgc-montpellier.fr/permutmatrix/. Accessed 24 May 2022
876 26. Warde-Farley D, Donaldson SL, Comes O, Zuberi K, Badrawi R, Chao P, et al. The GeneMANIA
877 prediction server: biological network integration for gene prioritization and predicting gene function.
878 Nucleic Acids Research. 2010;38(suppl_2):W214-W20.
879 27. GeneMANIA. https://genemania.org/. Accessed 18 May 2022
880 28. STRING. http://string-db.org. Accessed 22 June 2022
881 29. Szklarczyk D, Morris JH, Cook H, Kuhn M, Wyder S, Simonovic M, et al. The STRING database in
882 2017: quality-controlled protein-protein association networks, made broadly accessible. Nucleic Acids
883 Res. 2017;45(D1):D362-d8.
884 30. Pathan M, Keerthikumar S, Ang CS, Gangoda L, Quek CY, Williamson NA, et al. FunRich: An open
885 access standalone functional enrichment and interaction network analysis tool. Proteomics.
886 2015;15(15):2597-601.
887 31. Bell RD, Sagare AP, Friedman AE, Bedi GS, Holtzman DM, Deane R, et al. Transport pathways for
888 clearance of human Alzheimer's amyloid beta-peptide and apolipoproteins E and J in the mouse central
889 nervous system. Journal of cerebral blood flow and metabolism : official journal of the International
890 Society of Cerebral Blood Flow and Metabolism. 2007;27(5):909-18.
891 32. Berdowska I, Matusiewicz M, Krzystek-Korpacka M. HDL Accessory Proteins in Parkinson's
892 Disease—Focusing on Clusterin (Apolipoprotein J) in Regard to Its Involvement in Pathology and
893 Diagnostics—A Review. Antioxidants. 2022;11(3).
894 33. Emamzadeh FN, Allsop D. α-Synuclein Interacts with Lipoproteins in Plasma. Journal of
895 Molecular Neuroscience. 2017;63(2):165-72.
896 34. Arioz BI, Tufekci KU, Olcum M, Durur DY, Akarlar BA, Ozlu N, et al. Proteome profiling of
897 neuron-derived exosomes in Alzheimer's disease reveals hemoglobin as a potential biomarker.
898 Neuroscience Letters. 2021;755:135914.
899 35. Kitamura Y, Kojima M, Kurosawa T, Sasaki R, Ichihara S, Hiraku Y, et al. Proteomic Profiling of
900 Exosomal Proteins for Blood-based Biomarkers in Parkinson's Disease. Neuroscience. 2018;392:121-8.

901 36. Berdowska I, Matusiewicz M, Krzystek-Korpacka M. HDL Accessory Proteins in Parkinson's
902 Disease–Focusing on Clusterin (Apolipoprotein J) in Regard to Its Involvement in Pathology and
903 Diagnostics–A Review. Antioxidants. 2022;11(3).
904 37. Dal Magro R, Simonelli S, Cox A, Formicola B, Corti R, Cassina V, et al. The Extent of Human
905 Apolipoprotein A-I Lipidation Strongly Affects the β-Amyloid Efflux Across the Blood-Brain Barrier in
906 vitro. Frontiers in neuroscience. 2019;13:419.
907 38. Endres K. Apolipoprotein A1, the neglected relative of Apolipoprotein E and its potential role in
908 Alzheimer's disease. Neural Regeneration Research. 2021;16(11).
909 39. Fania C, Arosio B, Capitanio D, Torretta E, Gussago C, Ferri E, et al. Protein signature in
910 cerebrospinal fluid and serum of Alzheimer's disease patients: The case of apolipoprotein A-1
911 proteoforms. PLOS ONE. 2017;12(6):e0179280.
912 40. Paslawski W, Zareba-Paslawska J, Zhang X, Hölzl K, Wadensten H, Shariatgorji M, et al. α-
913 synuclein–lipoprotein interactions and elevated ApoE level in cerebrospinal fluid from Parkinson's
914 disease patients. Proceedings of the National Academy of Sciences. 2019;116(30):15226-35.
915 41. Paula-Lima AC, Tricerri MA, Brito-Moreira J, Bomfim TR, Oliveira FF, Magdesian MH, et al.
916 Human apolipoprotein A–I binds amyloid-β and prevents Aβ-induced neurotoxicity. The International
917 Journal of Biochemistry & Cell Biology. 2009;41(6):1361-70.
918 42. Qiang JK, Wong YC, Siderowf A, Hurtig HI, Xie SX, Lee VM-Y, et al. Plasma apolipoprotein A1 as a
919 biomarker for Parkinson disease. Annals of Neurology. 2013;74(1):119-27.
920 43. Song F, Poljak A, Crawford J, Kochan NA, Wen W, Cameron B, et al. Plasma Apolipoprotein
921 Levels Are Associated with Cognitive Status and Decline in a Community Cohort of Older Individuals.
922 PLOS ONE. 2012;7(6):e34078.
923 44. Swanson CR, Berlyand Y, Xie SX, Alcalay RN, Chahine LM, Chen-Plotkin AS. Plasma
924 apolipoprotein A1 associates with age at onset and motor severity in early Parkinson's disease patients.
925 Movement Disorders. 2015;30(12):1648-56.
926 45. van der Vorst EPC. High-Density Lipoproteins and Apolipoprotein A1. In: Hoeger U, Harris JR,
927 editors. Vertebrate and Invertebrate Respiratory Proteins, Lipoproteins and other Body Fluid Proteins.
928 Cham: Springer International Publishing; 2020. p. 399-420.

929 46. Zhou Q, Zhao F, Lv Z-p, Zheng C-g, Zheng W-d, Sun L, et al. Association between APOC1
930 Polymorphism and Alzheimer's Disease: A Case-Control Study and Meta-Analysis. PLOS ONE.
931 2014;9(1):e87017.
932 47. Castellano JM, Kim J, Stewart FR, Jiang H, DeMattos RB, Patterson BW, et al. Human apoE
933 Isoforms Differentially Regulate Brain Amyloid-β Peptide Clearance. Science Translational Medicine.
934 2011;3(89):89ra57-89ra57.
935 48. Deane R, Sagare A, Hamm K, Parisi M, Lane S, Finn MB, et al. apoE isoform-specific disruption of
936 amyloid beta peptide clearance from mouse brain. The Journal of clinical investigation.
937 2008;118(12):4002-13.
938 49. Merino-Zamorano C, Fernández-de Retana S, Montañola A, Batlle A, Saint-Pol J, Mysiorek C, et
939 al. Modulation of Amyloid-β 1–40 Transport by ApoA1 and ApoJ Across an in vitro Model of the Blood-
940 Brain Barrier. Journal of Alzheimer's Disease. 2016;53:677-91.
941 50. Verghese PB, Castellano JM, Garai K, Wang Y, Jiang H, Shah A, et al. ApoE influences amyloid-β
942 (Aβ) clearance despite minimal apoE/Aβ association in physiological conditions. Proceedings of the
943 National Academy of Sciences. 2013;110(19):E1807-E16.
944 51. Rye K-A, Clay MA, Barter PJ. Remodelling of high density lipoproteins by plasma factors.
945 Atherosclerosis. 1999;145(2):227-38.
946 52. Zhang X, Yin X, Yu H, Liu X, Yang F, Yao J, et al. Quantitative proteomic analysis of serum
947 proteins in patients with Parkinson's disease using an isobaric tag for relative and absolute
948 quantification labeling, two-dimensional liquid chromatography, and tandem mass spectrometry.
949 Analyst. 2012;137(2):490-5.
950 53. de Haan W, Out R, Berbée JFP, van der Hoogt CC, Dijk KWv, van Berkel TJC, et al. Apolipoprotein
951 CI inhibits scavenger receptor BI and increases plasma HDL levels in vivo. Biochemical and Biophysical
952 Research Communications. 2008;377(4):1294-8.
953 54. Berbée JFP, Vanmierlo T, Abildayeva K, Blokland A, Jansen PJ, Lütjohann D, et al. Apolipoprotein
954 CI Knock-Out Mice Display Impaired Memory Functions. Journal of Alzheimer's Disease. 2011;23:737-47.
955 55. Albert AD, Brad R. Parkinson disease and cognitive impairment. Neurology: Clinical Practice.
956 2016;6(5):452.

957 56. Fuior EV, Gafencu AV. Apolipoprotein C1: Its Pleiotropic Effects in Lipid Metabolism and
958 Beyond. International Journal of Molecular Sciences. 2019;20(23):5939.
959 57. Cudaback E, Li X, Yang Y, Yoo T, Montine KS, Craft S, et al. Apolipoprotein C-I is an APOE
960 genotype-dependent suppressor of glial activation. Journal of Neuroinflammation. 2012;9(1):192.
961 58. Abildayeva K, Berbée JFP, Blokland A, Jansen PJ, Hoek FJ, Meijer O, et al. Human apolipoprotein
962 C-I expression in mice impairs learning and memory functions. Journal of Lipid Research.
963 2008;49(4):856-69.
964 59. Association GAotWM. World Medical Association Declaration of Helsinki: ethical principles for
965 medical research involving human subjects. The Journal of the American College of Dentists.
966 2014;81(3):14.
967 60. Deutsch EW, Bandeira N, Perez-Riverol Y, Sharma V, Carver Jeremy J, Mendoza L, et al. The
968 ProteomeXchange consortium at 10 years: 2023 update. Nucleic Acids Research. 2022;51(D1):D1539-
969 D48.
970 61. Perez-Riverol Y, Bai J, Bandla C, García-Seisdedos D, Hewapathirana S, Kamatchinathan S, et al.
971 The PRIDE database resources in 2022: a hub for mass spectrometry-based proteomics evidences.
972 Nucleic Acids Research. 2021;50(D1):D543-D52.

(a)

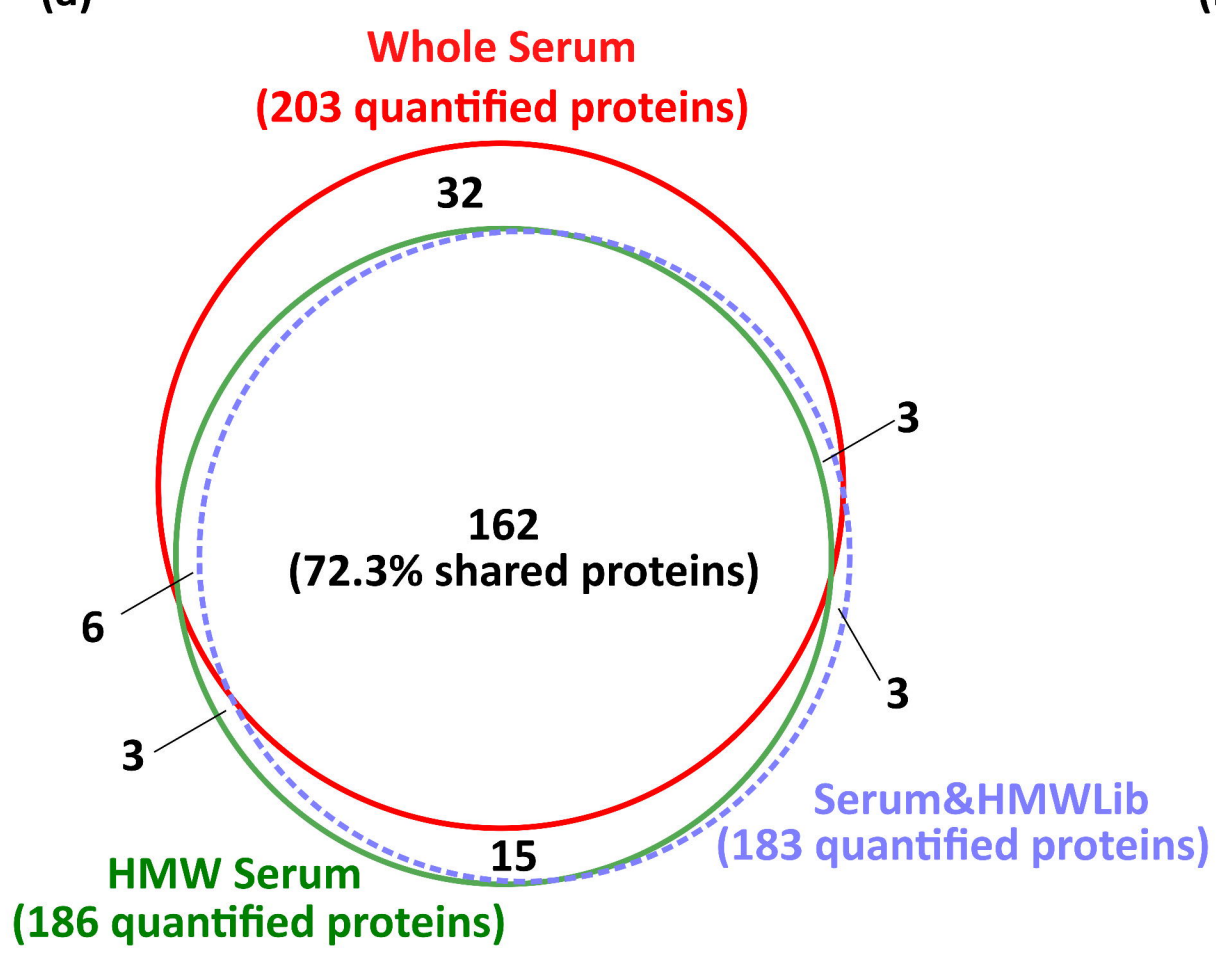

Total: 224 quantified proteins

(b)

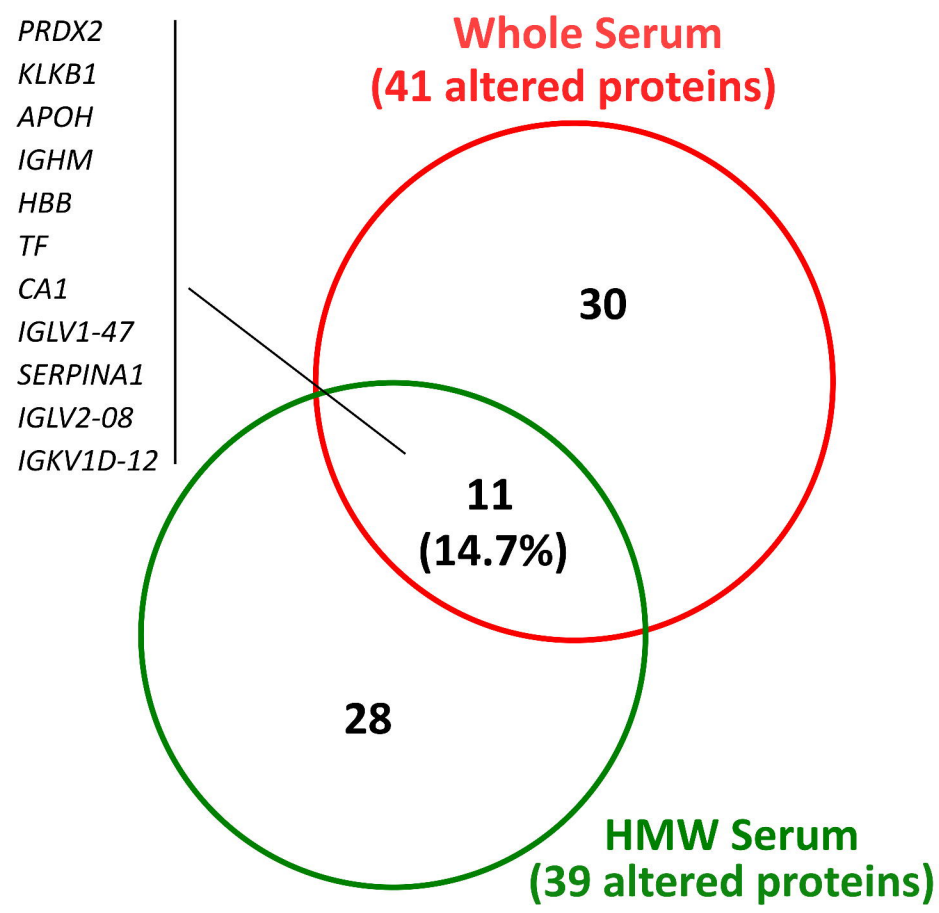

Total: 69 altered proteins

(c)

Group comparison	Gene Name	Protein Name	Fold Change Serum	Fold Change HMW
AD vs CT	*APOH*	Beta-2-glycoprotein 1 (APC inhibitor)	1.008#	0.676
	CA1	Carbonic anhydrase 1	2.467	2.397
	IGKV1D-12	Immunoglobulin kappa variable 1D-12	0.799	0.762
	IGLV1-47	*Immunoglobulin lambda variable 1-47*	0.767	0.786
	IGHM	Immunoglobulin heavy constant mu	0.372	0.692
	TF	Serotransferrin	0.856	0.792
	KLKB1	Plasma kallikrein	0.807	0.707
	PRDX2	*Peroxiredoxin-2*	2.691	2.979
	HBB	*Hemoglobin subunit beta*	3.958	3.129
PD vs CT	*SERPINA1*	Alpha-1-antitrypsin	0.877	0.752
AD vs PD	*APOH*	Beta-2-glycoprotein 1 (APC inhibitor)	1.238	0.803#
	CA1	Carbonic anhydrase 1	1.977	1.943
	IGLV1-47	*Immunoglobulin lambda variable 1-47*	0.894	0.785
	IGLV2-8	Immunoglobulin lambda variable 2-8	0.777	0.788
	PRDX2	*Peroxiredoxin-2*	1.749	2.568
	HBB	*Hemoglobin subunit beta*	2.622	2.094

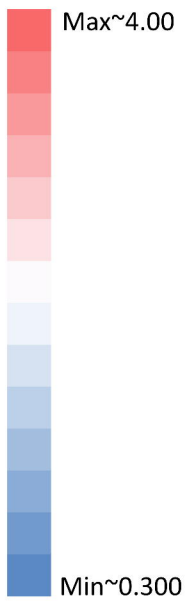

(a)

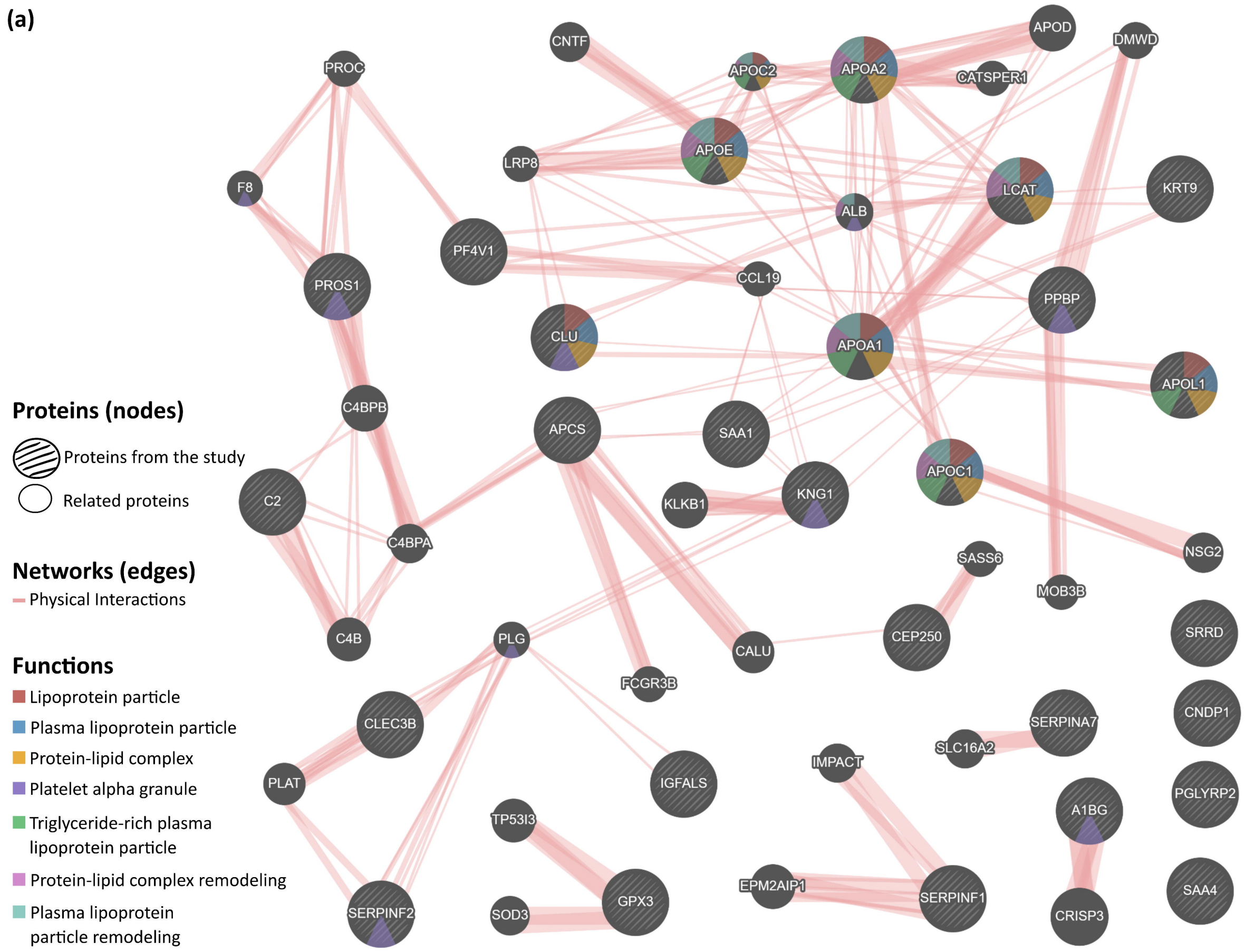
Proteins (nodes)
Proteins from the study
Related proteins
Networks (edges)
Physical Interactions
Functions
Lipoprotein particle
Plasma lipoprotein particle
Protein-lipid complex
Platelet alpha granule
Triglyceride-rich plasma lipoprotein particle
Protein-lipid complex remodeling
Plasma lipoprotein particle remodeling
CNTF
APOD
DMWD
PROC
APOC2
APOA2
CATSPER1
APOE
LRP8
F8
LCAT
KRT9
ALB
PF4V1
PROS1
CCL19
PPBP
CLU
APOA1
APOL1
C4BPB
APCS
SAA1
APOC1
C2
KLKB1
KNG1
C4BPA
NSG2
SASS6
MOB3B
C4B
PLG
CALU
CEP250
SRRD
FCGR3B
CLEC3B
SERPINA7
CNDP1
SLC16A2
IMPACT
PLAT
IGFALS
A1BG
PGLYRP2
TP53I3
EPM2AIP1
SERPINF1
SAA4
GPX3
SERPINF2
SOD3
CRISP3

(b)

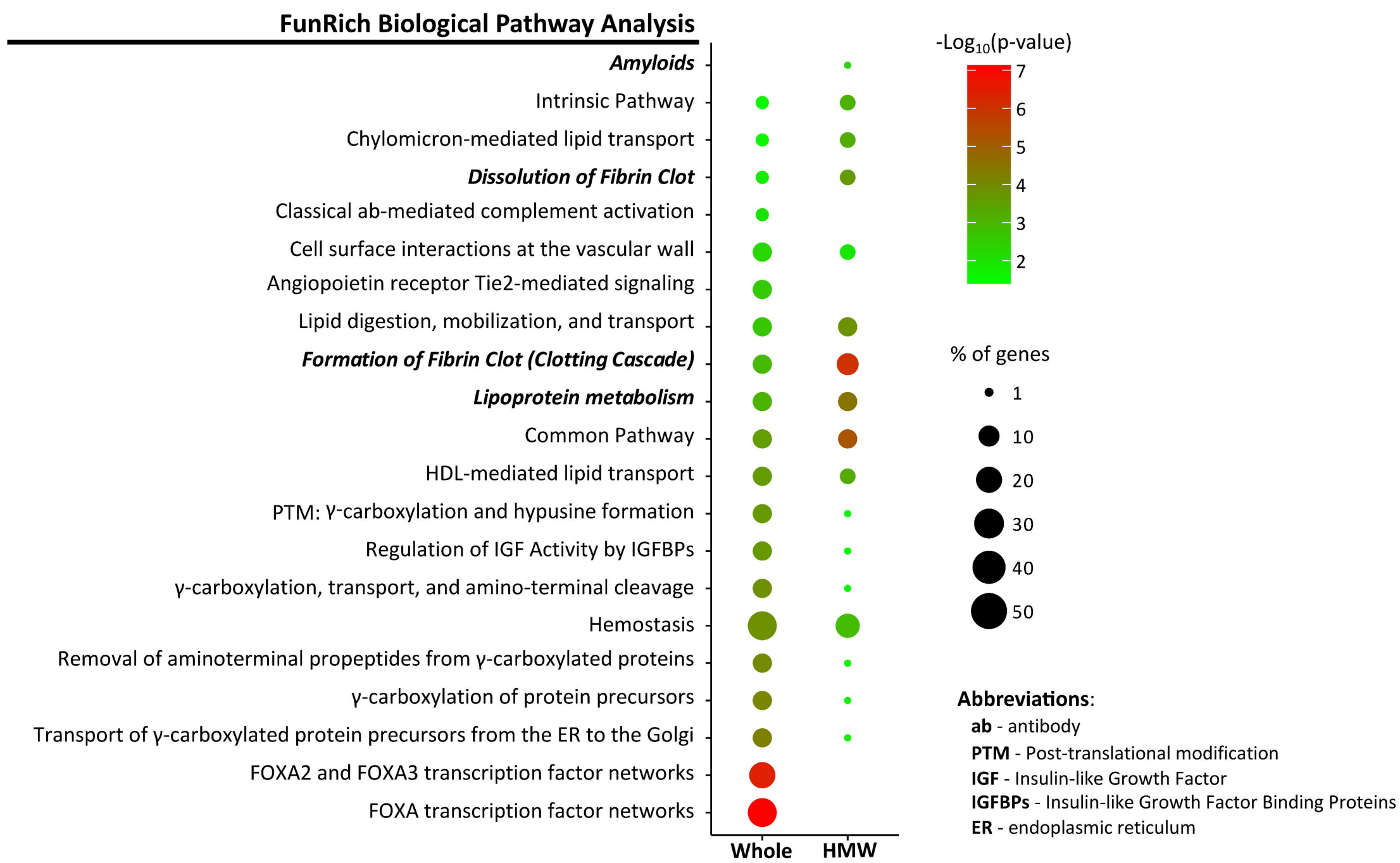
FunRich Biological Pathway Analysis
Amyloids
Intrinsic Pathway
Chylomicron-mediated lipid transport
Dissolution of Fibrin Clot
Classical ab-mediated complement activation
Cell surface interactions at the vascular wall
Angiopoietin receptor Tie2-mediated signaling
Lipid digestion, mobilization, and transport
Formation of Fibrin Clot (Clotting Cascade)
Lipoprotein metabolism
Common Pathway
HDL-mediated lipid transport
PTM: γ-carboxylation and hypusine formation
Regulation of IGF Activity by IGFBPs
γ-carboxylation, transport, and amino-terminal cleavage
Hemostasis
Removal of aminoterminal propeptides from γ-carboxylated proteins
γ-carboxylation of protein precursors
Transport of γ-carboxylated protein precursors from the ER to the Golgi
FOXA2 and FOXA3 transcription factor networks
FOXA transcription factor networks
Whole
HMW
-Log10(p-value)
7
6
5
4
3
2
% of genes
1
10
20
30
40
50
Abbreviations:
ab - antibody
PTM - Post-translational modification
IGF - Insulin-like Growth Factor
IGFBPs - Insulin-like Growth Factor Binding Proteins
ER - endoplasmic reticulum

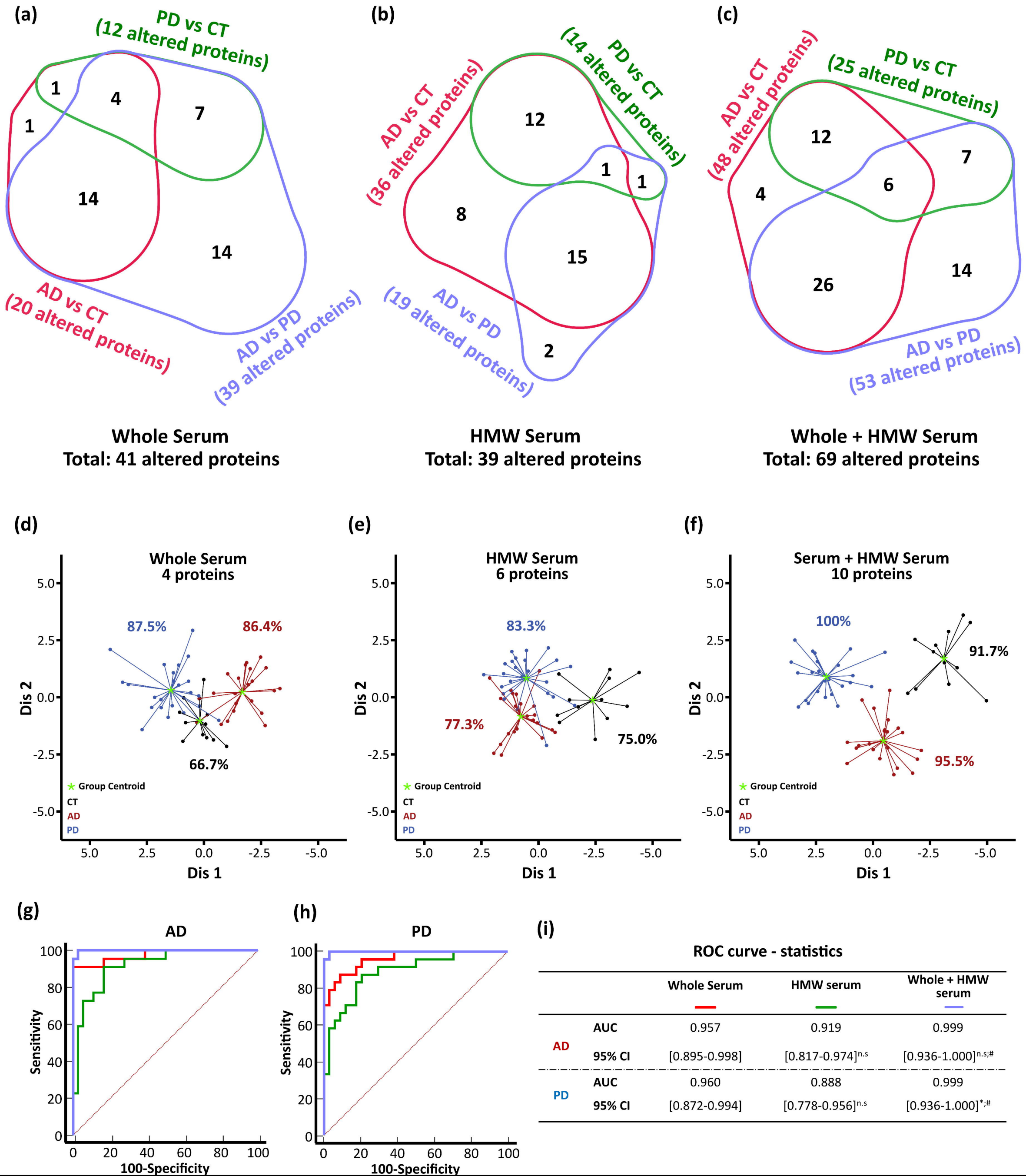

(i)

ROC curve - statistics

		Whole Serum	HMW serum	Whole + HMW serum
AD	AUC	0.957	0.919	0.999
	95% CI	[0.895-0.998]	[0.817-0.974]$^{n.s}$	[0.936-1.000]$^{n.s;\#}$
PD	AUC	0.960	0.888	0.999
	95% CI	[0.872-0.994]	[0.778-0.956]$^{n.s}$	[0.936-1.000]$^{*;\#}$

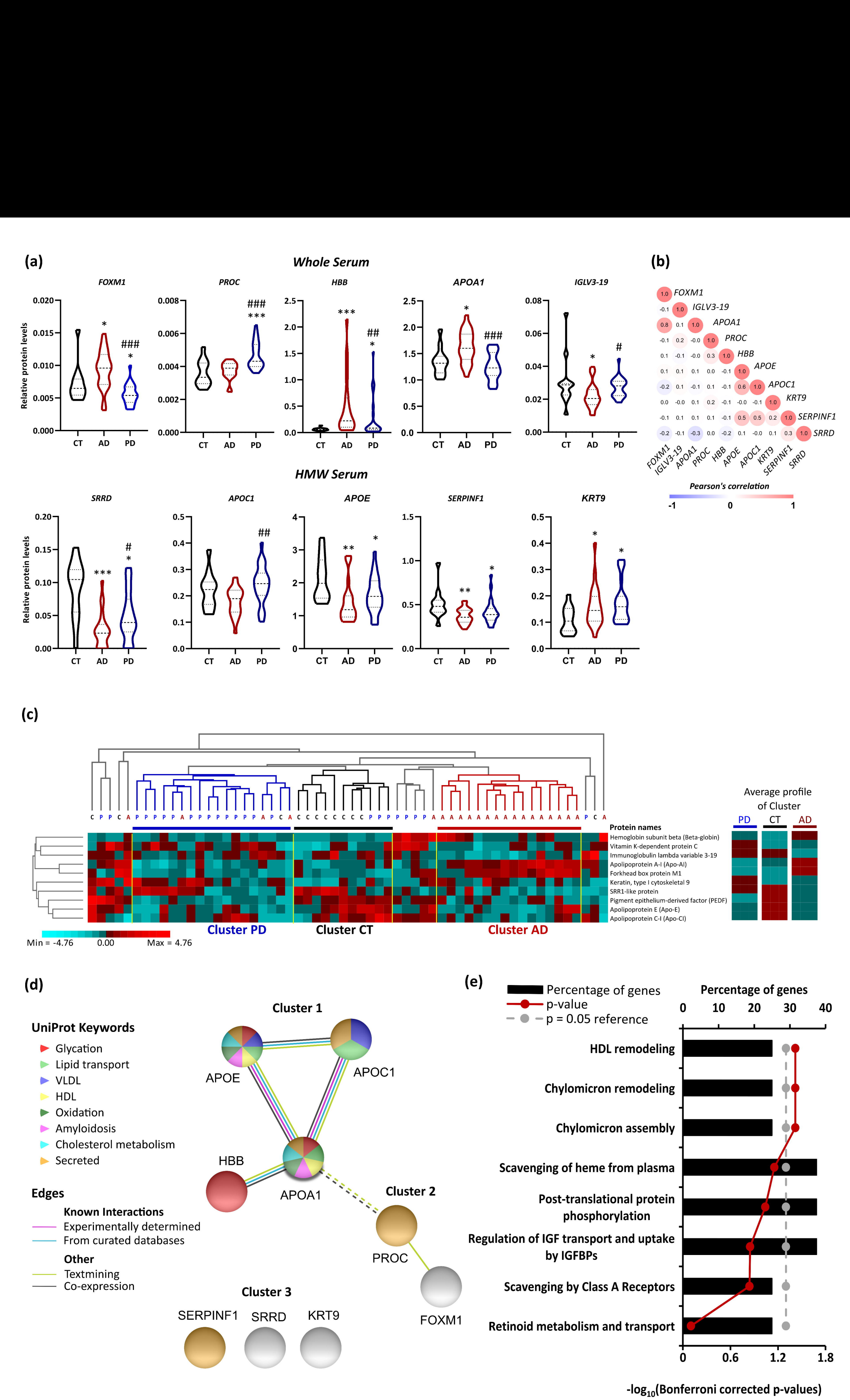
(a)
Whole Serum
FOXM1
PROC
HBB
APOA1
IGLV3-19
Relative protein levels
CT
AD
PD
HMW Serum
SRRD
APOC1
APOE
SERPINF1
KRT9
(b)
FOXM1
IGLV3-19
APOA1
PROC
HBB
APOE
APOC1
KRT9
SERPINF1
SRRD
Pearson's correlation
-1
0
1
(c)
Protein names
Hemoglobin subunit beta (Beta-globin)
Vitamin K-dependent protein C
Immunoglobulin lambda variable 3-19
Apolipoprotein A-I (Apo-AI)
Forkhead box protein M1
Keratin, type I cytoskeletal 9
SRR1-like protein
Pigment epithelium-derived factor (PEDF)
Apolipoprotein E (Apo-E)
Apolipoprotein C-I (Apo-CI)
Average profile of Cluster
PD
CT
AD
Cluster PD
Cluster CT
Cluster AD
Min = -4.76
0.00
Max = 4.76
(d)
UniProt Keywords
Glycation
Lipid transport
VLDL
HDL
Oxidation
Amyloidosis
Cholesterol metabolism
Secreted
Edges
Known Interactions
Experimentally determined
From curated databases
Other
Textmining
Co-expression
Cluster 1
APOE
APOC1
HBB
APOA1
Cluster 2
PROC
FOXM1
Cluster 3
SERPINF1
SRRD
KRT9
(e)
Percentage of genes
p-value
p = 0.05 reference
Percentage of genes
HDL remodeling
Chylomicron remodeling
Chylomicron assembly
Scavenging of heme from plasma
Post-translational protein phosphorylation
Regulation of IGF transport and uptake by IGFBPs
Scavenging by Class A Receptors
Retinoid metabolism and transport
-log10(Bonferroni corrected p-values)

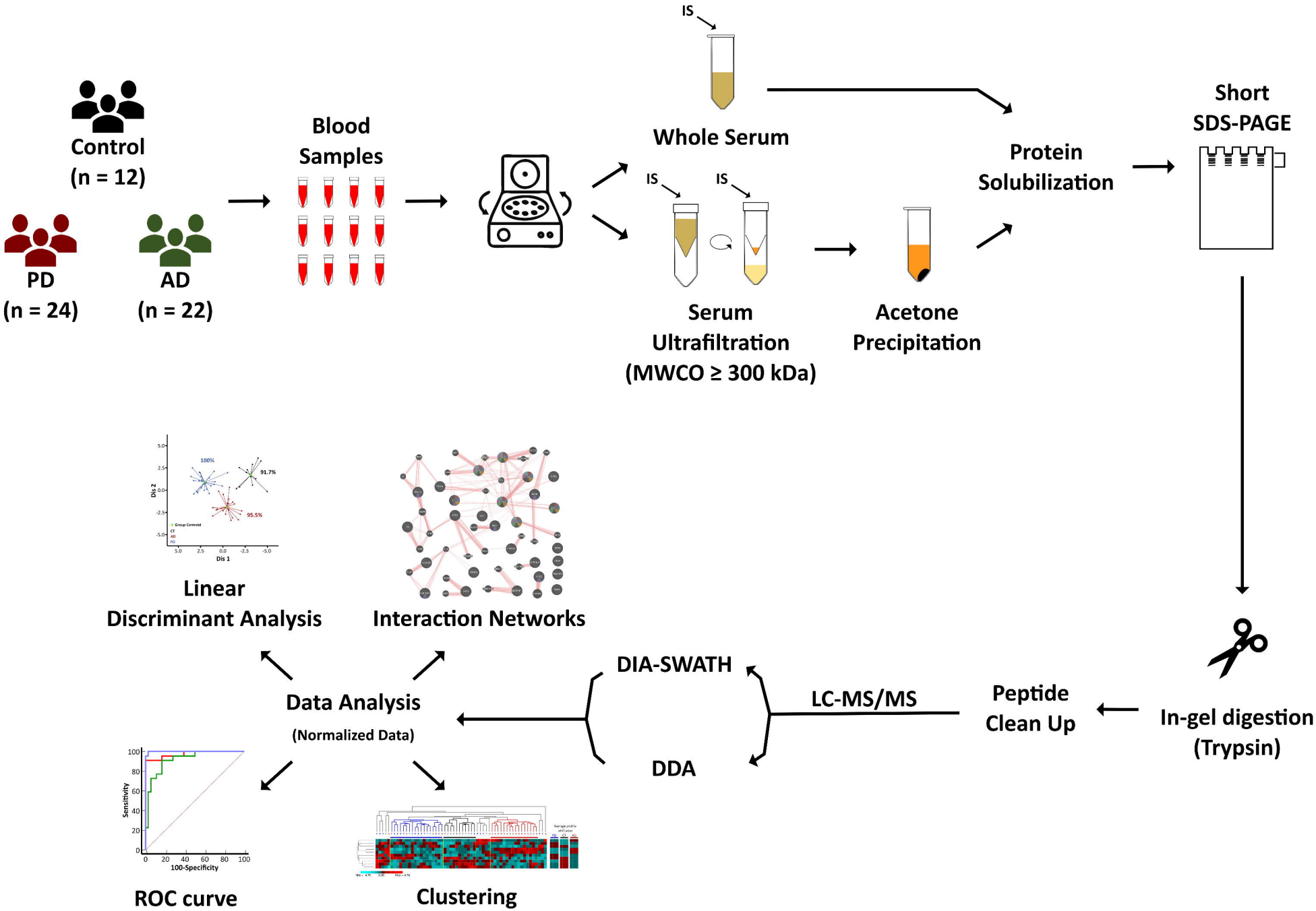
Control
(n = 12)
PD
(n = 24)
AD
(n = 22)
Blood
Samples
IS
Whole Serum
IS
IS
Serum
Ultrafiltration
(MWCO ≥ 300 kDa)
Acetone
Precipitation
Protein
Solubilization
Short
SDS-PAGE
In-gel digestion
(Trypsin)
Peptide
Clean Up
LC-MS/MS
DIA-SWATH
DDA
Data Analysis
(Normalized Data)
Linear
Discriminant Analysis
Interaction Networks
ROC curve
Clustering